

EARLY AND RAPID MERGING AS A FORMATION MECHANISM OF MASSIVE GALAXIES: EMPIRICAL CONSTRAINTS

CHRISTOPHER J. CONSELICE^{1,2}

Received 2004 October 27; accepted 2005 October 20

ABSTRACT

We present the results of a series of empirical computations regarding the role of major mergers in forming the stellar masses of modern galaxies based on measured galaxy merger and star formation histories from $z \sim 0.5$ to 3. We reconstruct the merger history of normal field galaxies from $z \sim 3$ to $z \sim 0$ as a function of initial mass using published pair fractions and merger fractions from structural analyses. We calibrate the observed merger timescale and mass ratios for galaxy mergers using self-consistent N -body models of mergers with mass ratios from 1:1 to 1:5 at various orbital properties and viewing angles. We use these simulations to determine the timescales and mass ratios that produce structures that would be identified as major mergers. Based on these calculations, we argue that a typical massive galaxy at $z \sim 3$ with $M_* > 10^{10} M_\odot$ undergoes $4.4^{+1.6}_{-0.9}$ major mergers at $z > 1$. We find that by $z \sim 1.5$ the stellar mass of an average massive galaxy is relatively established, a scenario qualitatively favored in a Λ -dominated universe. We argue that the final masses of these systems increase by as much as a factor of 100, allowing Lyman break galaxies, which tend to have low stellar masses, to become the most massive galaxies in today's universe with $M > M^*$. Induced star formation, however, only accounts for 10%–30% of the stellar mass formed in these galaxies at $z < 3$. A comparison to semianalytic models of galaxy formation shows that cold dark matter (CDM) models consistently underpredict the merger fraction, and rate of merging, of massive galaxies at high redshift. This suggests that massive galaxy formation occurs through more merging than predicted in CDM models, rather than a rapid early collapse.

Subject headings: galaxies: evolution — galaxies: interactions

1. INTRODUCTION

The prime motivation for studying galaxies at high redshift is to learn the history and physics responsible for their formation. The first step in this process is to identify galaxy populations in the distant universe. This has been accomplished to a degree with the discovery and systematic study of submillimeter sources (Blain et al. 2002), Ly α emitters (Kodaira et al. 2003), extremely red objects (Moustakas et al. 2004), and Lyman break galaxies (LBGs; Giavalisco 2002). The latter galaxies are UV-bright and star-forming, typically at $z > 2.5$, and are thus far the best studied high-redshift galaxy type. How these different galaxy populations are related to each other and to galaxies in the modern universe is a major area of research, and is still largely an open question. Another related issue is the history of the physical processes that drive galaxy formation, such as mergers, gas cooling, or some combination of these (Conselice et al. 2001). One fundamental problem is whether or not we have identified the progenitors of the most massive galaxies in the local universe at these early times. There are several indications that at least some massive galaxy progenitors are high-redshift LBGs. This includes clustering statistics showing that LBGs inhabit massive dark matter halos (e.g., Giavalisco et al. 1998; Adelberger et al. 1998, 2005). Other, possibly more massive and evolved galaxies exist at these redshifts, identified through infrared and submillimeter surveys, which may or may not be a subset of the LBG population (e.g., Franx et al. 2003; Chapman et al. 2003; Daddi et al. 2004). However, simple calculations show that the most massive galaxies today should be forming stars at $z \sim 3$, and it seems

likely that a subset of the LBG population is in some form the progenitors of a subset of modern massive galaxies.

There is, however, a problem with interpreting LBGs as the high-redshift progenitors of modern massive galaxies. LBGs are nearly as luminous as the most luminous galaxies in the nearby universe, yet they have stellar populations with low mass-to-light ratios (e.g., Papovich et al. 2001; Shapley et al. 2001), resulting in relatively low computed stellar masses. In fact, very few LBGs have stellar masses larger than the local value of M^* , the characteristic galaxy mass (Papovich et al. 2001; Shapley et al. 2001). These low mass-to-light ratios imply that there is considerable star formation in LBGs, and thus it is possible that extended star formation will produce galaxies with a large stellar mass by $z \sim 0$. However, when the observed ongoing star formation of LBGs is evolved to the present time, using reasonable assumptions, the resulting stellar masses are generally not large enough to be representative of massive galaxies in the nearby universe (Papovich et al. 2001). For LBGs to produce a large enough stellar mass by the time they evolve to $z \sim 0$, they must have multiple episodes of star formation, or somehow prolong or rejuvenate starbursts. Until recently, there has been no obvious way to determine if or when Lyman break galaxies will undergo future bursts.

One possible way for LBGs to increase their stellar mass and evolve into modern elliptical galaxies, or spiral bulges, is through the merger process (e.g., Conselice 2003b; Nagamine et al. 2005). Major mergers³ are efficient at triggering star formation as well as building up the stellar mass of a galaxy through the addition of mass from the “accreted” galaxy. The idea that LBGs are involved in major mergers has been suggested through theoretical

¹ California Institute of Technology, Mail Code 105-24, Pasadena, CA 91125.

² National Science Foundation Astronomy and Astrophysics Fellow.

³ A major merger is defined as a merger between two galaxies with a mass ratio of 1:3 or lower. A minor merger is between systems with a mass ratio higher than 1:3.

and empirical arguments (e.g., Somerville et al. 2001; Conselice et al. 2003a; Weatherley & Warren 2003), yet no detailed calculations have been performed to determine the number of mergers these systems go through, or how much mass is potentially added to LBGs due to this process.

We examine the evidence for major mergers at high redshift in this paper and calculate, based on empirical data, how many mergers a typical $z \sim 3$ galaxy undergoes as a function of redshift, finding that a typical massive galaxy undergoes on average $4.4_{-0.9}^{+1.6}$ major galaxy mergers. This is an extension of our earlier work, where the merger fraction is derived using deep *Hubble Space Telescope* (*HST*) imaging of the Hubble Deep Field (Conselice et al. 2003a). This new paper presents a reanalysis of these merger fractions and includes N -body models to calibrate timescales in which galaxies would be seen as mergers through their structures. This allows us to produce the first galaxy merger rates and merger histories at $z > 1$. We furthermore use the observed stellar masses of galaxies undergoing major mergers to determine the average stellar mass accumulation due to mergers as a function of mass, and as a function of time. We also derive the amount of star formation likely induced by these mergers. We conclude that due to the merger process LBGs can become the most massive galaxies in today's universe through the major merger process, and most of this formation is complete by $z \sim 1.5$. We compare our empirical predictions with observations of how the stellar masses of galaxies grow with time, and with specific predictions from cold dark matter based models.

Throughout this paper we use the following cosmology: $H_0 = 70 \text{ km s}^{-1} \text{ Mpc}^{-1}$, $\Omega_\Lambda = 0.7$, and $\Omega_m = 0.3$. In § 2 we summarize the various data used in this paper to perform the calculations, § 3 is an analysis of merger fractions and rates, and their evolution, including a new fitting formalism, and § 4 contains a calculation of how many mergers a high-redshift galaxy will undergo and how much stellar mass is added during this process, while § 5 is a discussion of our results and § 6 is a summary.

2. DATA AND METHODS

To constrain the role of mergers in forming galaxies requires understanding the merger history through pair and structural methods and the measured stellar masses of $z \sim 3$ galaxies. These data come from many sources, as we require constraints on the merger and mass assembly history of galaxies out to $z \sim 3$. Merger fractions and histories derived using pairs of galaxies (§ 3.1) come from Patton et al. (2000, 2002), Le Fèvre et al. (2000), and Lin et al. (2004) at $z < 1$. We use previously published and cataloged data from Conselice et al. (2003a, 2005a) for galaxy mergers at $z > 0.5$ that use galaxy structural information from the Hubble Deep Field North and South. We also use the stellar masses calculated and tabulated for high-redshift ($z > 2$) galaxies to constrain the initial masses for these mass growth calculations (e.g., Papovich et al. 2001).

We present merger fractions as a function of redshift for galaxies at $z > 1$ based on galaxies seen in the Hubble Deep Field North (HDF-N) and South (HDF-S). We identify mergers in Conselice et al. (2003a) and in this paper through the CAS (concentration, asymmetry, clumpiness) system (Conselice 2003a; Conselice et al. 2002). The basic idea behind CAS morphologies is that galaxies undergoing major mergers can be identified through their large asymmetries measured in the rest-frame optical band (Conselice et al. 2000c; cf. Windhorst et al. 2002; Papovich et al. 2003 for the UV). The merger fractions for galaxies in the HDF-N up to $z \sim 3$ are discussed in detail in Conselice et al. (2003a). We present a new analysis here using data from both the HDF-N and HDF-S, particularly through deep Near-Infrared Camera and

Multi-Object Spectrometer (NICMOS) imaging of the HDF-N for high- z systems in § 3.1.4 (also see Dickinson et al. 2000).

3. ANALYSIS

3.1. Merger Fraction Evolution

3.1.1. Definitions

We define the galaxy merger fraction f_{gm} as the number of galaxies undergoing a merger (N_{gm}) divided by the total number of galaxies (N_T) within a given redshift (z), stellar mass (M_*), or (\vee) luminosity (M_B) range,

$$f_{\text{gm}}(z, M_B \vee M_*) = \frac{N_{\text{gm}}}{N_T}. \quad (1)$$

This differs from previous studies, such as morphological methods and pair methods, where the merger fraction is defined as the number of mergers (N_m) divided by the total number of galaxies. It may appear that these two are the same quantity; however, they are not, as a merger by definition involves the conglomeration of two or more galaxies. Our definition of f_{gm} is more general, can be easily calculated from the pair definition, and is directly translated into merger rates using the timescale of a merger. Since usually $N_{\text{gm}} = 2N_m$, the galaxy merger fraction can be converted into a merger fraction simply by multiplying by a factor of 2 for merger fractions computed in pair studies.

The galaxy merger fraction can be directly computed through a morphological method using the observed number of mergers (N_m) and the total number of observed galaxies (N_T) by

$$f_{\text{gm}} = \frac{N_m \kappa}{N_T + (\kappa - 1)N_m}, \quad (2)$$

where κ is the average number of galaxies that merged to produce the N_m mergers and must be ≥ 2 . We only use values of $\kappa = 2$ in this paper. The observational method for determining N_m , and the tabulated values, are discussed in Conselice et al. (2000a, 2000b), Bershady et al. (2000), and Conselice (2003a, 2003b).

3.1.2. Merger Fractions at $z < 0.3$

The pair and merger fraction at $z \sim 0$ sets the baseline for understanding all other higher redshift merger fractions, and it is worth spending some time trying to determine it and the corresponding merger rate. When discussing merger fraction and merger rates, it is imperative to be very specific about the selection criteria and the luminosities or masses of the galaxies under study, as the merger fraction changes as a function of mass and luminosity in both the nearby and distant universe (Conselice et al. 2003a; Xu et al. 2004).

The traditional method for finding mergers is to search for systems in pairs and to quantify this by the pair fraction, f_p . This has been effectively applied up to redshifts $z \sim 1$ (e.g., Carlberg et al. 1994; Le Fèvre et al. 2000; Patton et al. 2002; Bundy et al. 2004; Lin et al. 2004). Using Sloan Digital Sky Survey (SDSS) data, the merger fraction for close pairs, with an average galaxy luminosity of $M_{g^*} = -20.13$, was computed as 0.5% (Allam et al. 2004). A similar merger fraction is found by examining galaxies in pairs using Two Micron All Sky Survey (2MASS) data (Xu et al. 2004). Other studies, such as the use of the UGC catalog of nearby galaxies, have found that the merger fraction of galaxies is similar to these values, $f_m = 2.1\% \pm 0.2\%$ (Patton et al. 1997).

Patton et al. (2000) used a redshift survey of nearby galaxies to determine the merger fraction at $z \sim 0$ using new merger quantifiers, N_c and L_c , which are the average number of pairs per

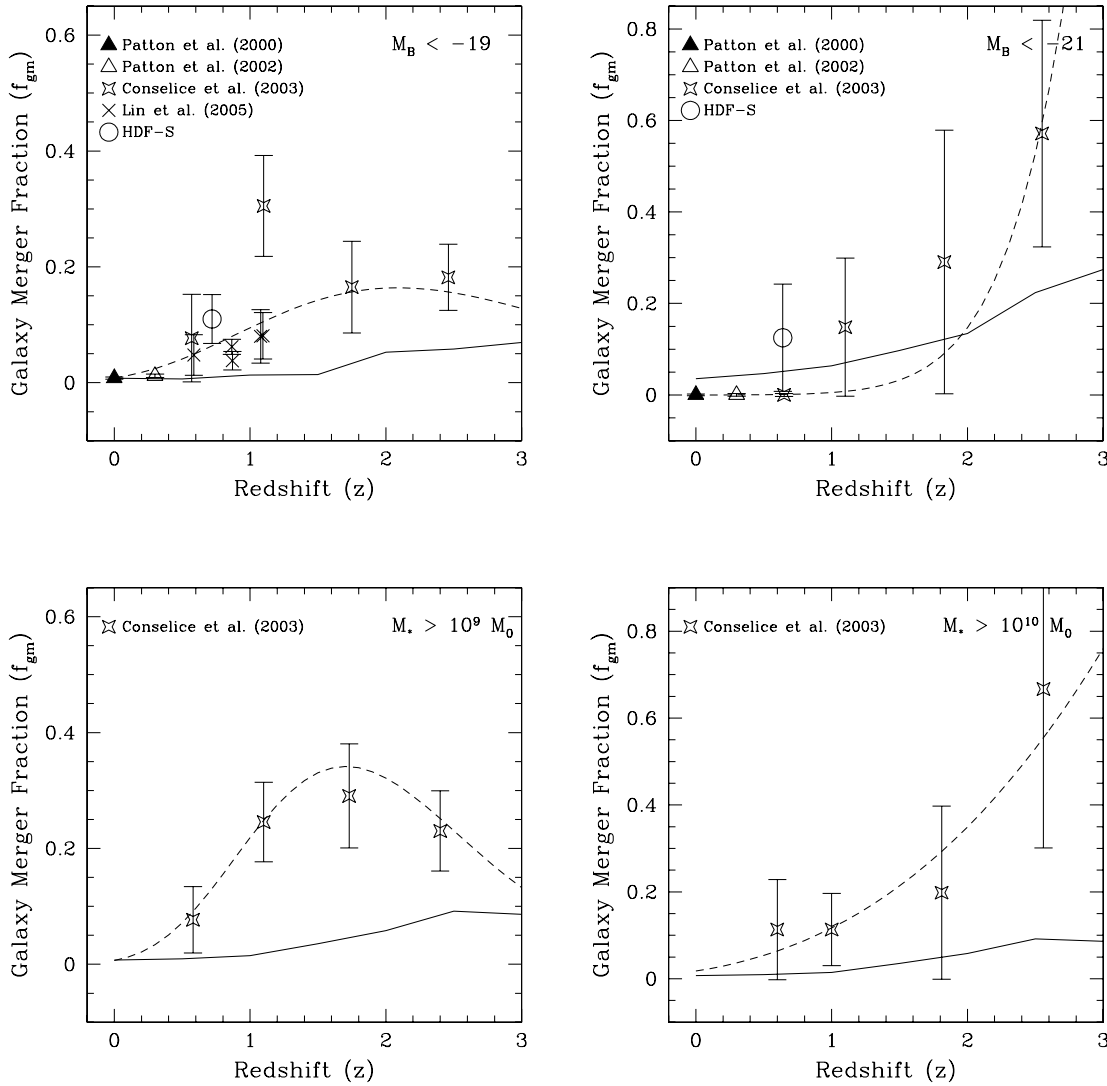


FIG. 1.—Merger fraction at two different luminosity limits, $M_B < -19$ (top left) and $M_B < -21$ (top right), and two upper mass limits, $M_* > 10^9 M_\odot$ (bottom left) and $M_* > 10^{10} M_\odot$ (bottom right). Plotted are merger fractions from pair counts and morphological measures from Patton et al. (2000, 2002), Conselice et al. (2003a), and Lin et al. (2004). The dashed lines are the best fit to the merger fractions, where a power law of the form $f_{\text{gm}} = f_0(1+z)^m$ is fitted for the systems with $M_B < -21$ and $M_* > 10^{10} M_\odot$ and a power law/exponential of the form $f_{\text{gm}} = \alpha(1+z)^m \exp[\beta(1+z)]$ is fitted for systems with $M_B < -19$ and $M_* > 10^9 M_\odot$. The solid line shows CDM model predictions for mergers occurring within these luminosities and stellar masses.

galaxy (N_c) and the average luminosity of these pairs per galaxy (L_c). Furthermore, Patton et al. (2000) show that the vast majority of galaxies with companions are pairs, and therefore $f_p = 2N_c$. However, only a fraction of these pairs will merge, and Patton et al. (2000) calculate that at $z \sim 0$ about half of all the observed pairs will do so. At high redshifts the fraction likely to merge increases as $(1+z)$ (e.g., Le Fèvre et al. 2000).

On Figure 1, we plot merger fractions, derived from pairs at $z \sim 0$ systems taken from Patton et al. (2000) at luminosities $M_B < -19$ and $M_B < -21$. Patton et al. (2002) find that pair fractions and the value of N_c increase for fainter systems, and are effectively zero at bright ($M_B < -20$) magnitude limits. We convert N_c into our f_{gm} by multiplying by 2 to account for the second galaxy involved in the merger, and divide by 2 to account for the relative fraction of pairs that are likely to merge (Patton et al. 2000). Thus, in our formalism $f_{\text{gm}}(z=0) = N_c(z=0)$.

3.1.3. Merger Fractions from $0.3 < z < 1$

The merger fraction and rate was first deduced to have been higher in the past using simple arguments in Toomre (1977). The first measurements of the merger fraction at high redshift, as

opposed to simply inferring the evolution in the merger fraction (Zepf & Koo 1989), were performed by Carlberg et al. (1994). These early merger studies were done by finding pairs that were separated by various angular sizes, usually $6''$ or so (Zepf & Koo 1989). A major result from Carlberg et al. (1994) and others (e.g., Patton et al. 1997) was that the pair fraction is around 3 times higher at $z \sim 0.4$ than it is today. These studies characterized the merger fraction evolution as a power law with redshifts, $f_m = f_0(1+z)^m$, with fitted power-law indices $m \sim 3-4$.

Patton et al. (1997) used the now standard definition of pairs as systems with a separation of $20 h^{-1}$ kpc, or less, and found a pair fraction at $z \sim 0.33$ of $4.7\% \pm 0.9\%$, while at $z \sim 0$ the fraction is $2.1\% \pm 0.2\%$. In other studies, merger fractions were reported to be similar, although there are some who find a shallower rise in the pair fraction up to $z \sim 1$ (Carlberg et al. 2000; Lin et al. 2004). Much of this discrepancy can be accounted for by the different luminosity ranges used and assumptions for how to account for luminosity evolution (Patton et al. 2002; Lin et al. 2004).

Patton et al. (2002), using the formalism for mergers outlined in Patton et al. (2000; § 3.1.2), computed values of $N_c = 0.012 \pm 0.003$ for galaxies brighter than $M_B = -19$ at $z \sim 0.3$. As at

$z \sim 0$, the value of N_c declines at brighter magnitude limits. Other methods for determining the pair and merger fraction up to $z \sim 1$ include Le Fèvre et al. (2000) and Lin et al. (2004), who find similar results.

The derived galaxy merger fractions found in these pair studies are plotted on Figure 1. The increase is well fitted by a $(1+z)$ power law, giving indices $m = 2-4$, consistent with most theoretical predictions of how merger fractions decline with redshift (e.g., Gottlober et al. 2001). However, due to the onset of the Hubble sequence, it is likely that most merging activity is over by $z \sim 1$ for massive galaxies (Conselice et al. 2005b). Since 50%–75% of the stellar mass in galaxies is formed by $z \sim 1$ (e.g., Dickinson et al. 2003), it is critical to try to place constraints on the formation modes for galaxies at earlier times.

3.1.4. Merger Fractions at $z > 1$

Merger fractions at $z > 1.2$ are currently all determined through morphological methods (Conselice et al. 2003a; Lotz et al. 2004). The merger fraction is determined through the use of equation (2), which includes determining the observed number of galaxies likely to be mergers through a particular computational method. In this paper, we use the CAS system to identify galaxies that are likely undergoing major mergers at all redshifts (see Conselice 2003a). Conselice et al. (2003a) present the detailed reasoning behind these computations, as well as the $z > 1.5$ data we use in this paper.

All morphological methods identify a number of “morphological mergers” (N_{morph}) that must be converted into the number of actual mergers (N_m) by

$$N_m = N_{\text{morph}} \frac{f_1}{f_2}, \quad (3)$$

where f_1 is the fraction of galaxies identified as a merger that are actual mergers, and f_2 is the fraction of actual mergers picked up by the morphological method. In Conselice et al. (2003a) it was assumed that $f_1/f_2 = 1$, which for the reasons below, we use here as well.

The CAS system identifies major mergers through the use of the asymmetry (A ; Conselice 1997; Conselice et al. 2000b) and clumpiness parameters (S ; Conselice 2003a). The assumptions we make in using these two parameters are that (1) the structures of galaxies have a physical meaning, (2) star formation occurs in clumps, as it does in the nearby universe (Lada & Lada 2003), and (3) a galaxy that has a large-scale asymmetry indicates a non-equilibrium dynamical state and is likely undergoing a major merger. These assumptions are well established for nearby galaxies (Conselice 2003a) and are likely valid at higher redshifts as well. The quantitative criteria used to determine whether a galaxy is a merger at $z = 0$ is

$$(A_{\text{optical}} > 0.35) \wedge (A_{\text{optical}} > S_{\text{optical}}), \quad (4)$$

where \wedge is the operation definition of “and.” Galaxies with $A > 0.35$ in the nearby universe are about 99% mergers, and thus $f_1 \sim 1$ at $z \sim 0$. The second criterion in equation (4) is important, as galaxies can be asymmetric because of star formation as well as from the presence of a merger (Conselice et al. 2000b). However, galaxies dominated by star formation, and which are not merging, have large clumpiness and asymmetry values because the light is distributed in localized and compact star-forming complexes (Conselice 2003a; Mobasher et al. 2004). We therefore use the clumpiness index (S) to remove star-forming

galaxies from consideration as a merger by the above criteria. If a galaxy has a high asymmetry, but a low clumpiness value, it implies that the asymmetric light is not localized, but is a large-scale feature indicating that the system is not virialized. The criterion for this is simply $A > S$. Not all galaxies involved in a major merger are identified through this process, yet the simulations discussed in § 3.3 suggest that all major mergers are asymmetric at some point in their evolution. Thus, $f_2 \sim 1$, although it would be lower if we considered mergers within a given timescale.

Merger fractions at $z > 1$ are presented in Conselice et al. (2003a), although we reevaluate these using equation (2) to obtain the galaxy merger fraction. Galaxy merger fractions computed using two magnitude ($M_B < -19$, $M_B < -21$) and mass ($M_* > 10^9 M_\odot$, $M_* > 10^{10} M_\odot$) limits are shown in Figure 1. We assume throughout that $\kappa = 2$ (eq. [2]). The merger fractions computed through the CAS system at $z \sim 1$ are within 1σ of the merger fractions computed using the pair fraction method (Conselice et al. 2003a). The most interesting and important feature of these merger fractions is that they become quite large at high redshift for the most luminous and most massive galaxies (Conselice et al. 2003a), with $f_{\text{gm}} = 0.5-0.7$ at $z \sim 2.5$. The implication from this is that the merger rate is very high for these systems, and that this might be a way to form modern galaxies.

3.1.5. Fitting the Merger Fraction

Figure 1 plots all published galaxy merger fractions available to date for mergers at two luminosities, $M_B < -21$ and $M_B < -19$, and two stellar mass limits, $M_* > 10^{10} M_\odot$ and $M_* > 10^9 M_\odot$. Note that this is an inhomogeneous data set, as the timescale in which these fractions are valid can vary by a substantial amount. However, we later show that these timescales are similar for both the pair and the merger method (§ 3.3) and thus can be compared fairly.

Traditionally, the evolution of merger fractions with redshift is fitted by a power law of the form $f_m = f_0(1+z)^m$, where f_0 is the merger fraction at $z = 0$ and m is the power-law index. Fits of m using this formalism have varied from $m = 0$ to 4 up to $z \sim 1$, although most studies find values that are around $m = 2-4$ (cf. Bundy et al. 2004; Lin et al. 2004 when examining mergers in the near-infrared, and when accounting for luminosity evolution). It is worthwhile to examine whether a power-law history, which is quickly becoming the standard way to characterize the merger fraction evolution, is in fact the appropriate formalism.

Fitting the merger fraction by a power law was initially motivated by the theory of structure formation. By assuming that primordial density perturbations are Gaussian, the resulting merging history of dark halos can be understood based on the Press-Schechter (P-S; Press & Schechter 1974) formalism. Press & Schechter describe how the density of dark matter halos of mass M evolves as a function of time. The P-S formalism, and its extension (Bond et al. 1991; Bower 1991; Lacey & Cole 1993), agree well with N -body models of the hierarchical galaxy formation process (e.g., Gottlober et al. 2001) and have been used as the basis for all semianalytic CDM models, some of which have published these merger histories (Kolatt et al. 2000; Gottlober et al. 2001; Khochfar & Burkert 2001).

Based on the output of these simulations, the fraction of galaxies merging is well approximated by the $(1+z)^m$ formalism up to about $z \sim 2$. The m index contains much information, including the value of the primordial power-law index (n), the cosmological constant, and the matter density parameter (Ω_m ; Carlberg 1991). The merger fraction, however, does not appear to be well fitted by a power law empirically out to $z \sim 3$ (Conselice et al. 2003a), especially for lower mass and fainter systems. One

fitting function with some theoretical basis is a mixed power-law, exponential function,

$$f_{\text{gm}}(z) = \alpha(1+z)^m \exp[\beta(1+z)], \quad (5)$$

where the $z=0$ merger fraction is given by $f_{\text{gm}}(z=0) = \alpha \exp(\beta)$. An analytic formulation of the merger fraction gives a similar form based on the P-S theory (Carlberg 1990), and equation (5) is in fact often a better fit than a $(1+z)$ power law.

We fit values of α , β , and m from equation (5) for the galaxy merger fraction in the mass and luminosity bins used in Conselice et al. (2003a). We find $\alpha = 0.2\text{--}0.6$, $\beta = -1.5$ to -3.7 , and $m = 5\text{--}10$ for systems with $M_* < 10^{10} M_\odot$. We also fit the traditional $(1+z)^m$ fitting formalism, although only up to $z \sim 1.5$, or $z \sim 1$ for all but the brightest and most massive bins. We find that the merger fraction out to $z \sim 1\text{--}2$ can be well fitted by a power law with power-law indices $m = 2\text{--}4$ for all galaxy types.

There are a few additional points about the merger fraction history that should be noted. The first is that for $M_* < 10^{10} M_\odot$ and $M_B > -20$ galaxies there appears to be a peak turnover redshift around $z_{\text{turn}} \sim 1.5\text{--}2$, where the galaxy merger fraction declines at $z > z_{\text{turn}}$ (Fig. 1; Conselice et al. 2003a). This redshift can be computed analytically through $df_{\text{gm}}/dz = 0$, or $z_{\text{turn}} = -1/(m/\beta + 1)$, where we compute $z_{\text{turn}} = 1.5\text{--}2.5$ for galaxies with $M_* < 10^{10} M_\odot$ and $M_B > -21$. There does not appear to be a turnover redshift for the most luminous ($M_B < -21$) and most massive ($M > 10^{10} M_\odot$) galaxies up to $z \sim 3$, although they must flatten off at some higher unknown redshift.

3.2. Merger Rates

Using the merger fraction in a physical context requires that we understand the timescale in which a merger is occurring and thus convert the galaxy merger fraction f_{gm} into a galaxy merger rate (\mathcal{R}), defined within a redshift, luminosity, and mass range. The formalism for this is

$$\mathcal{R}(z, M_B, M_*) = f_{\text{gm}} \tau_m^{-1} n_m, \quad (6)$$

where τ_m is the timescale for a merger to occur and n_m is the comoving or physical density of all galaxies within a given luminosity or mass range and at a given redshift. Determining τ_m is critical for using the observed galaxy merger fraction, and for determining the importance of galaxy mergers for forming galaxies. Since the timescale of a merger is too long to observe directly, we must use theoretical arguments and models to determine the timescale of major mergers. The comoving or physical density n_m can be determined from observations of the galaxy luminosity or mass function (Papovich et al. 2001; Shapley et al. 2001) or by directly counting the number of galaxies within a luminosity or mass bin in the sample under study. If the former method is used, it is critical that the selection method be identical to the method for finding mergers. We use two methods, described below, for determining the timescale of a merger: dynamical friction arguments and N -body models of the merging process.

3.2.1. Dynamical Friction Timescales

The typical method for determining the merger timescale of two galaxies is the dynamical friction argument. This is based on the assumption that galaxies are embedded in dark matter halos. We revisit this computation here, although a more detailed analysis requires the use of simulations, which we discuss in § 3.3.

To compute the time required for two galaxies to merge necessitates that we make some assumptions. The first is that the

mass profiles of galaxies are isothermal with a mass distribution that falls off as r^{-2} . Based on this, there is a fictional drag force that induces angular momentum loss. As such, the two galaxies will gradually approach each other until they merge. The time for two galaxies, separated by r_i , to be separated by $r_f < r_i$ is

$$t_{\text{fric}} = 0.0014 \text{ Gyr} \left(r_i^2 - r_f^2 \right) \left(\frac{v_c}{100 \text{ km s}^{-1}} \right) \left(\frac{10^{10} M_\odot}{M} \right), \quad (7)$$

where v_c is the relative velocity between the two galaxies, M is the mean accreted mass, and where we have assumed the Coulomb logarithm, $\ln \Lambda = 2$, based on equal mass merger simulations (Dubinski et al. 1999; Patton et al. 2000). For the velocity (v_c) and mass quantities (M), we take the average values from Patton et al. (2002), finding $v_c = 260 \text{ km s}^{-1}$ and $M \sim 3 \times 10^{10} M_\odot$, although these values will change when considering galaxies of different masses and luminosities. Using these fiducial values, and the projected radii of a given pair, we calculate the timescale for a merger to occur, or rather for the pair's separation to change from r_i to r_f .

We use equation (7) as the timescale for the merger rate for galaxies in pairs. Typically, we find that the time for a merger to occur by equation (7) is $0.5\text{--}1$ Gyr, although the exact value changes under different assumptions. This is one reason why pair fraction methods are very difficult to convert into a physically meaningful quantity. Throughout this paper we assume that the derived merger timescales for galaxy pairs have an associated systematic uncertainty of 0.25 Gyr. The structural method, using the properties of galaxies after they have merged, has the potential to be more robust for quantifying the timescale of a merger, and thus also the merger rate.

3.3. N -Body Models of Galaxy Mergers

The above argument reveals that the merger timescale for two galaxies of similar mass is roughly 0.5 Gyr. Our goal in this section is to understand whether we can do better than this estimate using the structures of galaxies and the timescale in which a galaxy will be identified as a merger structurally. To determine the time- and mass-scale sensitivity of galaxy structures to mergers, we carry out and analyze a series of N -body models of galaxies undergoing mergers. These models are described in detail in, e.g., Mihos & Hernquist (1996), Dubinski et al. (1999), and Mihos (2001).

The models we use are composed of dark matter and stars. We do not include the morphological effects of star formation in these simulations, as modeling this aspect is very difficult with an infinite number of possibilities, whose reflection of actual properties is doubtful and is not straightforward to model. To test the effect of star formation, we place fake star-forming complexes in these simulations by hand, which does increase the measured asymmetry. The clumpiness index, however, also increases, such that the effective asymmetry $\sim(A - S)$ matches the asymmetry before placing these star-forming complexes in the N -body simulations (§ 3.1.4).

The techniques and detailed descriptions of these models can be found in Hernquist (1993) and Mihos & Hernquist (1996). Each of the N -body models is composed of 294,912 luminous (nondark matter) and 65,536 dark matter particles, and is modeled using the TREE SPH hierarchical tree (Hernquist 1987). Most of our models are composed of bulges and disks, with a bulge-to-disk ratio of 1:3, while others are pure disks. The dark matter halos in these simulations are isothermal spheres with core radii equal to the scale length of each model's disk. The dark matter halo is truncated at radii larger than 10 times the core radius, with an exponential decline (Hernquist 1993). The mass of the

disk in these simulations is $M_d = 1$, with a bulge mass of $M_b = \frac{1}{3}$ and a halo mass of $M_h = 5.8$, all in simulation units. Scaling to the Milky Way, this gives a total mass of $3.2 \times 10^{11} M_\odot$ and a model disk scale length of 3.5 kpc. The ratios of the total masses for the simulated galaxy pairs in the merger simulations are 1:1, 1:2, 1:3, and 1:5. We analyze images of these simulations using snap shots separated by 26 Myr. For each simulation we analyze a total of 61 snapshots from the beginning of the simulation until ~ 1.5 Gyr. We analyze 10 different simulations (listed in Table 1) at seven different viewing angles each.

We study these N -body simulations using the same structural techniques used to study galaxies at high and low redshift using the CAS morphological analysis techniques. For three mass ratios (1:1, 1:2, and 1:3) we simulate mergers with a mix of the following orbital properties: inclined, retrograde, and prograde. The prograde simulation contains one disk inclined by 20° to the orbital plane, while the inclined simulation has a 75° inclination, and the retrograde is at a 135° inclination. The three simulations at each mass include one galaxy that is inclined and another that is retrograde (IR), one galaxy that is prograde and another that is inclined (PI), and simulations with one galaxy prograde and the other retrograde (PR). Figure 2 shows a graphical representation of the 1:1 IR simulation.

We carry out CAS measurements on these simulations in three different ways, each designed to match how these values are measured on actual galaxies. Different measurement methods are important to consider, as the resulting values of the CAS parameters can vary depending on how the galaxies were detected and cataloged. The three main issues are the following: (1) When galaxies are merging, are they detected in the same SExtractor segmentation area (Conselice et al. 2003a, 2004, 2005b)? (2) When measuring the CAS parameters during the merger, do you remove the second galaxy? (3) Where the center is placed can change the outcome of the CAS measurements.

All of these points deserve discussion, although they are inherently related to each other. The process for measuring the CAS parameters for a galaxy involves two steps, and because the next generation of morphological analyses will involve at least tens of thousands of galaxies, this process must be automated. We have therefore considered various approaches for measuring the CAS parameters on these simulations. The detection process on *Hubble Space Telescope* imaging almost universally involves the SExtractor program, which detects and splits galaxies using significance thresholds. Usually the way this is fine-tuned is to separate galaxies by trial and error using the detection and separation parameters. However, it is inevitable that close galaxies will sometimes be placed in the same detection. The prevalence of this needs to be determined by examining galaxies by eye that are asymmetric, although details of this process are beyond the scope of the current paper.

However, there are situations in which two galaxies are close enough during a merger that they should be considered the same system. In Conselice (2003a) it is argued that the extent of a galaxy should be defined as the light within the Petrosian radius. If there are two interacting galaxies, which are spatially close, then wherever the Petrosian radius converges determines whether or not those two galaxies should be considered the same system or not. In this situation the center of the system will be between the two centers of the merging galaxies. As such, we also consider this center when performing CAS measurements, determining the asymmetry timescale for each scenario.

We list the timescale information for simulations at a representative viewing angle of 54° , the results of which are listed in Table 1 as $\tau_{\text{sim}1} - \tau_{\text{sim}4}$, which we abbreviate as $\tau_1 - \tau_4$. This is the

TABLE 1
MERGER MODEL TIMESCALES

Simulation	$\tau_{\text{sim}1}$ (Gyr)	$\tau_{\text{sim}2}$ (Gyr)	$\tau_{\text{sim}3}$ (Gyr)	$\tau_{\text{sim}4}$ (Gyr)
1:1 IR	0.96	0.5	0.57	0.29
1:1 PI	0.65	0.31	0.29	0.23
1:1 PR	0.78	0.42	0.39	0.26
1:1 NoB	0.86	0.57	0.78	0.81
1:2 IR	1.04	0.44	0.34	0.26
1:2 PI	0.83	0.39	0.26	0.21
1:2 PR	0.86	0.31	0.36	0.21
1:3 IR	0.70	0.42	0.31	0.18
1:3 PI	0.75	0.44	0.23	0.23
1:3 PR	0.73	0.47	0.41	0.21

NOTES.—This table describes the various timescales in which different N -body simulations would be identified as an ongoing major merger through the CAS system. The different simulations are for systems with mass ratios of 1:1, 1:2, and 1:3 at three different orbital inclinations (IR, PI, and PR; see text). The different timescales are listed as sim1 through sim4. These simulations are the timescales for the different possible ways of computing the CAS indices. The first two timescales (sim1, sim2) are when the CAS indices are measured when both galaxies are imaged, with sim1 when the center was placed between the two galaxies merging and sim2 when it was placed on the center of the more massive system. The value of sim3 is the timescale for a merger computed within the CAS system after the fainter galaxy is removed from the image and only the massive system is measured, and sim4 is when the massive galaxy is removed and only the less massive system is measured. The values of sim3 and sim4 accurately represent how the CAS parameters are being measured on actual data (Conselice et al. 2004) and are what we use in this paper.

time in which the simulated galaxies are asymmetric enough to be considered a major merger using the same criteria used on high-redshift galaxies. Another scenario we consider is when the center of the CAS run is placed on the brightest galaxy's center and when the fainter galaxy or pair is not removed. The time in which this pair will be seen as an asymmetric merger, with $A > 0.35$, is listed in Table 1 as τ_2 .

Very often however, what occurs in the SExtractor process is that two galaxies are separated into different systems. The CAS code has an option, which is now being used (e.g., Conselice et al. 2004), to remove all galaxies from an image not currently being analyzed. We are then left with a single galaxy. To mimic this method we only image one galaxy at a time in our simulation and measure its CAS parameters. This is effectively the same approach used in Conselice et al. (2003a), where the CAS values were measured within the area given by the segmentation maps. Neighboring galaxies were, however, not removed, similar to the sim2 simulations whose timescales we use in § 3.3.4 to obtain merger rates. One result of the “galaxy removal” simulations is shown in Figure 3, where the asymmetry, concentration, and size measurements for the brightest galaxy in a merging pair are shown as a function of time in the 1:1 IR simulation (Fig. 2). To determine the effects of viewing angle on these timescales, we viewed the merger simulations at viewing angles of 15° , 54° , 77° , 90° , 117° , 145° , and 165° , finding the same result to within 0.2 Gyr.

There are several observations to take away from Figure 3. The first is that for the 1:1, 1:2, and 1:3 simulations each galaxy starts with a low asymmetry and a high concentration. In the 1:1 simulation, as the two galaxies start to interact, at about 0.4 Gyr (see Fig. 2), the structures become more asymmetric. For an interval of ~ 0.2 Gyr these galaxies remain asymmetric enough due to this encounter to be identified as an asymmetric merging galaxy. After the initial encounter, the galaxies separate and contain a lower asymmetry until 1 Gyr into the simulation, when

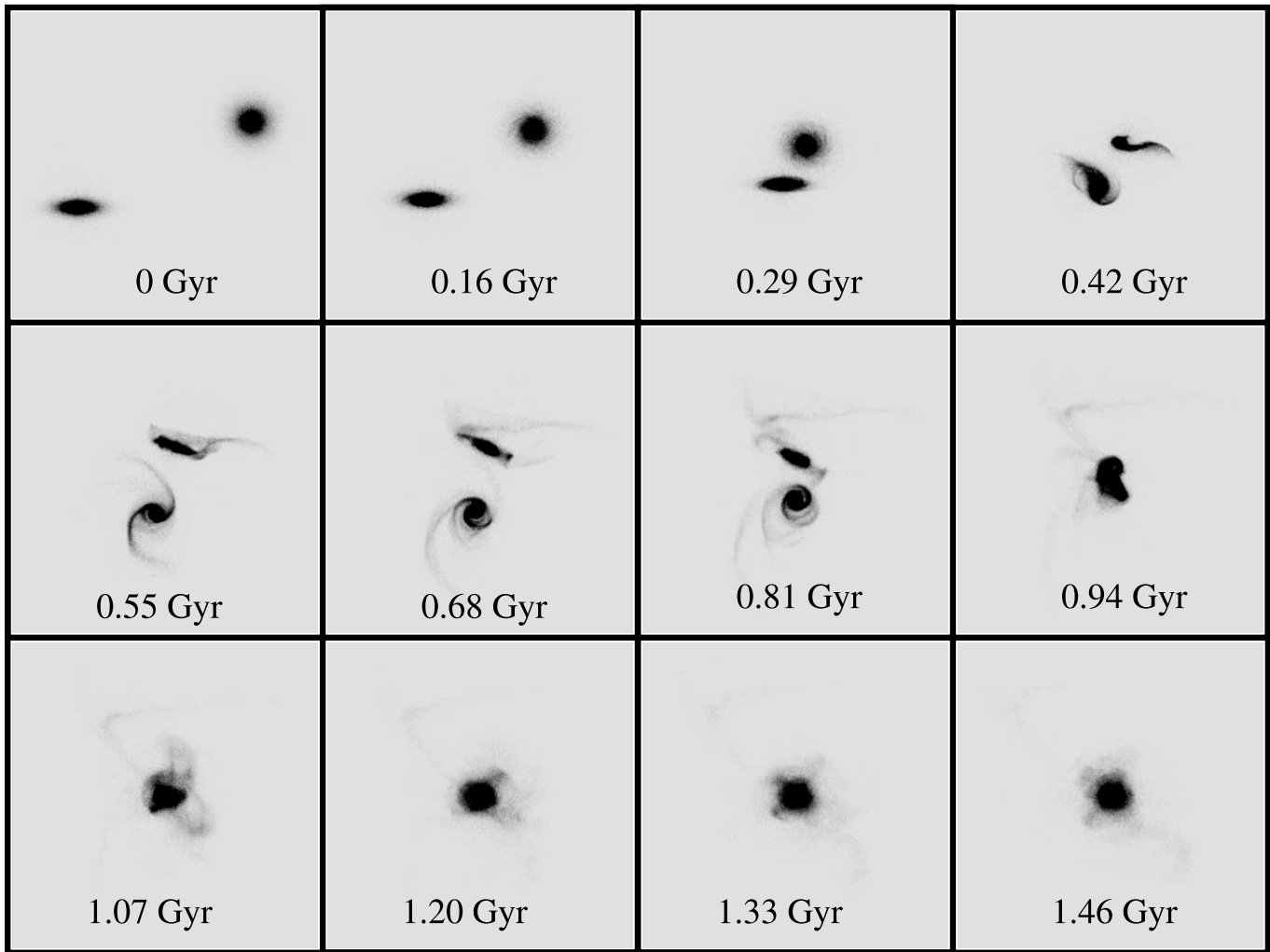


FIG. 2.—Visual realization of a 1:1 merger simulation analyzed in this paper. The time at the bottom of each frame is the time during the simulation up until 1.46 Gyr.

both galaxies become asymmetric for another 0.2–0.3 Gyr. At about 1.3 Gyr the two systems have completely merged, and the merger remnant has cooled enough dynamically to have a low structural asymmetry. Note that from Figure 3 the asymmetry evolution of the 1:1 simulation is to first order independent of orbital type (Table 1). Some variation does exist; for example, the 1:1 IR simulation has a delayed asymmetry response during the second peak, although this does not change the derived effective merger timescale.

The CAS merger timescale sensitivity for the more massive galaxy in this configuration (τ_3), with the lower mass galaxy not imaged, is tabulated in Table 1. The listed values of τ_4 are the CAS merger timescales for the lower mass of the pair, when the more massive system is not imaged. We find that the two times are nearly identical, that is, the timescale is independent of mass and mass ratio up to 1:3. The averages and 1σ ranges in the time intervals in which the asymmetry index is sensitive to finding a merger are $\tau_1 = 0.82 \pm 0.12$, $\tau_2 = 0.43 \pm 0.08$, $\tau_3 = 0.29 \pm 0.20$, and $\tau_4 = 0.29 \pm 0.19$. The 1σ systematic ranges quoted for these different time intervals are taken from the values in Table 1. They thus include ranges in mass ratio and orbital properties, but do not include systematic effects from different viewing angles, which add another 0.1 Gyr uncertainty. Note that these 1σ systematic ranges are not proper 1σ error measurements on the timescales in which galaxies at high redshift will merge.

They are only the 1σ range in the merger timescales for the galaxy simulations that we study, which likely does not represent the real range in these galaxies.

3.3.1. Pure Disk Simulations

The simulations discussed in § 3.3 are for galaxies with a 1:3 bulge-to-disk ratio. The merger timescale can vary if the structures of galaxies are different from the bulge/disk ratios we assumed for our initial galaxies. As such, we perform a 1:1 simulation of two pure disk galaxies, the results of which are shown in Table 1 as 1:1 NoB. We find that the pure disk galaxy simulations are asymmetric enough to be counted as a merger for a longer period of time than galaxies with bulges, by as much as a factor of 2. This is the case when we consider the simulations in which only one galaxy is considered (τ_3 and τ_4) as well as when both galaxies are used in the CAS computations (τ_1 and τ_2). The reason for this is that these pure disks do not decrease in asymmetry after the first encounter. The presence of a bulge is a stabilizing entity that creates a lower asymmetry when the two simulated galaxies are in the process of merging. This creates some uncertainty in the timescale for the merger, although as discussed in § 3.3.3, this effect is not likely to be large when we consider the numerous mergers a massive galaxy undergoes and the likely formation of bulgelike systems in massive galaxies by $z \sim 3$ (Baugh et al. 1996; Ferguson et al. 2004).

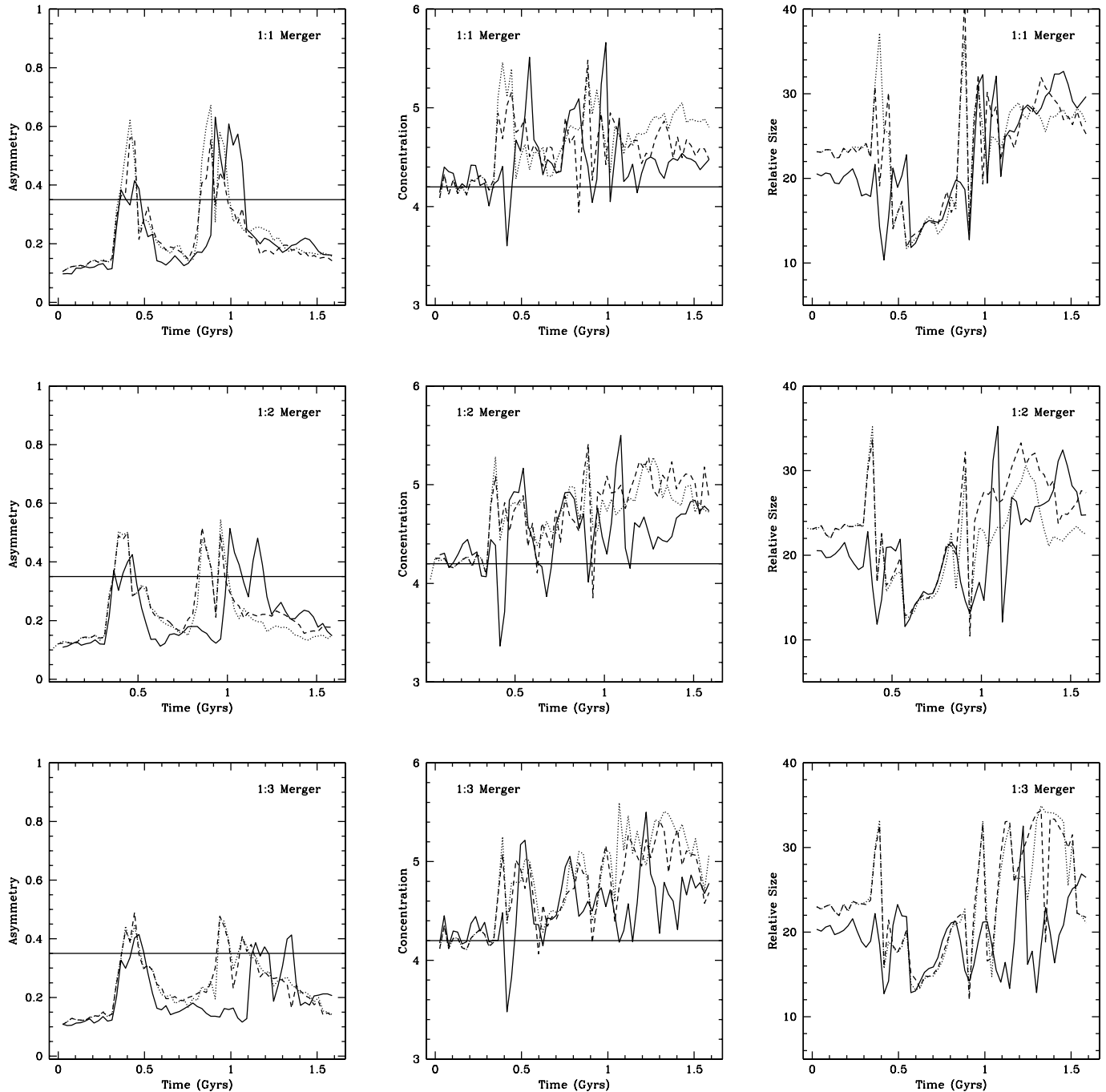


FIG. 3.—Evolution of the asymmetry, concentration, and sizes for galaxies in our N -body simulations. The three dashed lines are for simulations with different types of orbits, with the IR (solid line), PI (dashed line), and PR (dotted line) models shown. The solid line in the asymmetry diagram is the limit for finding galaxy mergers (Conselice 2003a). The solid line in the concentration diagram shows an average value for bulge-dominated galaxies.

3.3.2. Minor Merger Simulations

We investigate a minor merger model,⁴ a 1:5 mass ratio merger, whose resulting asymmetry, concentration, and size as a function of time are shown in Figure 4. The most obvious result of this simulation is that neither galaxy ever obtains an asymmetry value high enough to be considered a major merger. The two galaxies do not effectively merge until 3.5 Gyr into the

⁴ Observationally, a minor merger is typically a merger that has a mass ratio greater than 1:3 or 1:4, although dynamicists usually consider a galaxy with a 1:5 ratio an intermediate mass merger, and only mergers with mass ratios of 1:10 or greater, a minor merger.

simulation, when the asymmetry becomes high, but just shy of the $A = 0.35$ limit for a merger at $z = 0$. The timescale for this minor merger to complete is much longer than the lower mass ratio major mergers, with a total merger time of >4 Gyr. Since the age of the universe at $z > 2$ is small (3.3 Gyr), it is unlikely that a single minor merger can produce the high asymmetry signal seen in high-redshift galaxies. Although, we caution that more extensive simulations of lower mass ratio mergers with different initial conditions are needed to fully determine the generality of this. This simulation also likely does not match the initial conditions of galaxies in pairs and the distributions of orbital energies for high- z pairs, which are currently unknown. We also cannot rule

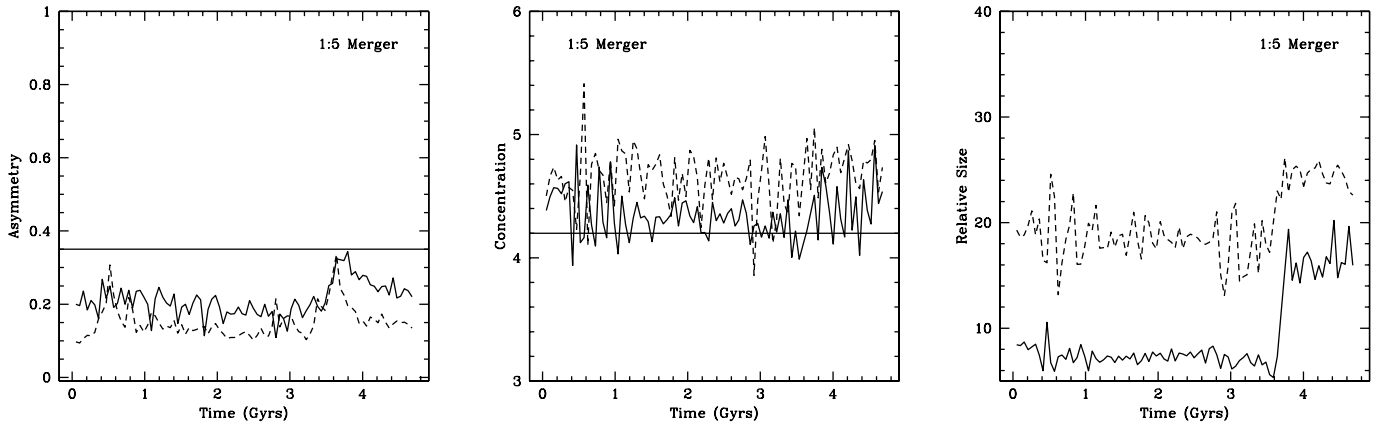


FIG. 4.—Similar to Fig. 3, but for mergers that have a mass ratio of 1:5. The lines are the same as in Fig. 3, except that in this case the two lines that represent the simulations (*solid and dashed lines*) are the asymmetry (A), concentration (C), and size values for the simulated (less and more massive of the pair) galaxies.

out the possibility that multiple minor mergers are occurring at once to produce a large asymmetry signal. More N -body models of different merger scenarios are necessary to address these issues.

From the analysis in this section we conclude that the mergers of galaxies with mass ratios higher than 1:5 are not likely to be producing a merger signal through the asymmetry index. If this is indeed the case, and we assume it is for the remainder of this paper, then it implies that the CAS method for finding mergers is a powerful approach that is insensitive to minor mergers, even a 20% mass merger. This is further confirmed empirically through observations of galaxies in pairs in the local universe (Hernandez-Toledo et al. 2005).

3.3.3. Limits on the N -Body Models

The simulations we examine above are necessarily limited and only offer a subset of the possible variety of conditions experienced by galaxies undergoing mergers/interactions at high redshift. It is currently not feasible to perform a more general analysis than the above, as a full suite of self-consistent N -body simulations with all possible initial conditions does not yet exist. The simulations we examine are low-speed encounters with isothermal dark matter profiles. However, we consider several other possibilities, including high-speed encounters between galaxies, galaxies with dark matter profiles that differ from isothermal, and galaxies mergers that have different masses than the nominal Milky Way mass considered here.

First, high-speed encounters between galaxies have been modeled by Moore et al. (1998) through “galaxy harassment.” These interactions can result in significant mass loss (Conselice 2002), and are likely ongoing in clusters today (Conselice & Gallagher 1999; Gregg & West 2004; Adami et al. 2005). This may also be an important process for forming dwarf galaxies. However, these encounters do not produce a significant morphological disturbance in a galaxy. Over time, harassment can destroy disks, but this process has a timescale much longer than the lifetimes of the morphological disturbances we measure with the asymmetry index. These high-speed impulsive encounters increase the internal energy of the interacting systems, which results in a galaxy that physically expands, but does so in a uniform manner. We therefore consider it an unlikely possibility that very high speed galaxy encounters can produce a large asymmetry signal that we would identify as a major merger.

Another complication is that galaxy interactions that do not necessarily merge can potentially create a large asymmetry that would be miscounted as a merger. These false-positive mergers

are unlikely, based on several arguments. The first is that empirically only nearby galaxies that are within a radius of each other produce a large asymmetry signal (Hernandez-Toledo et al. 2005). As these nearby pairs are within a few 10s of kpc of each other and have very small velocity differences, they are in the processes of merging, as they simply do not have a high enough velocity to escape. Galaxies that are interacting, but are not as close as a scale length, do not have asymmetry values in the merger regime (Hernandez-Toledo et al. 2005). These results are also suggested by our N -body models, where a similar pattern is seen. Furthermore, if high-redshift galaxies have an initial velocity difference that is large, and therefore repeated “flybys” occur until a final merger takes place, only the low-velocity encounters will produce a large asymmetry. Based on our models, we include only one flyby. However, we consider in the analysis in § 3.3.4 the asymmetry merger timescale becoming larger due to more than one flyby.

A further complication in these models is that the mass of the most massive system is similar to that of the Milky Way. The dynamical friction timescale for two galaxies to merge is largely independent of the mass ratio of the two galaxies, as long as they can be considered pointlike particles. However, once the two systems begin to interact strongly, the timescale can vary (Hernandez & Lee 2004). After the two galaxies merge, the relaxation timescale (τ_{relax}) depends on the density of the merger remnant, such that

$$\tau_{\text{relax}} = (R^3/GM_{\text{dyn}})^{1/2} \propto (1/G\rho)^{1/2}.$$

Using the fundamental plane relation, we know that the luminosity of a galaxy is proportional to a factor (β) of its velocity dispersion, or

$$L \propto \sigma^\beta.$$

N -body models suggest that merger remnants follow this relationship (e.g., Capelato et al. 1995; Aceves & Velazquez 2005; Boylan-Kolchin et al. 2005). Using the relationship $M_{\text{dyn}} \propto \sigma^2 R$ and the fact that $L = (L/M_{\text{dyn}})M_{\text{dyn}}$, we can write the ratio of the relaxation timescale for merger remnants at two different masses as

$$\frac{\tau_{\text{relax}}}{\tau'_{\text{relax}}} = \left(\frac{M_{\text{dyn}}}{M'_{\text{dyn}}}\right)^{1-(3/\beta)} = \left(\frac{M_{\text{dyn}}}{M'_{\text{dyn}}}\right)^{1/4}, \quad (8)$$

assuming that the ratio L/M_{dyn} is independent of M_{dyn} . By using the value $\beta = 4$ found through the Sloan Digital Sky Survey (Bernardi et al. 2003), we obtain the second part of equation (8), or that the timescale increases as $M_{\text{dyn}}^{1/4}$. This suggests that the asymmetry timescale during relaxation from a merger has a weak dependence on the total mass. We account for this dependence in § 3.3.4.

Finally, it is possible that the dark matter halos of galaxies at high redshift are different from the ones used in our simulations. One possibility is that the dark matter profile is less steep and denser than an isothermal profile, such that the dynamical friction timescale is shorter. Using a variety of reasonable possible dark matter profiles, Mihos et al. (1998) and Dubinski et al. (1999) investigate how different profiles will change the structure of tidal tails and features in merger galaxies. These papers, particularly Dubinski et al. (1999), show that extended profiles do not produce tidal tails; however, the inner parts of these galaxies are distorted due to the merger, irrespective of the dark matter profile, and this is the part of the galaxy that contributes the most to the asymmetry signal. We have not analyzed these simulations, since the parameter space of possible dark matter halo profiles at high redshift is infinite, as there are currently no observational constraints. It therefore remains an unaccounted for systematic effect in our merger timescales.

3.3.4. Computed Merger Timescales and Rates

We can use the above information to determine a few very important quantities that have up until now been largely unknown. The first is the time in which two galaxies merging will be identified as a merger within the CAS system. In § 3.3 we describe the total amount of time our simulated galaxies appear asymmetric, yet we can divide this time further into the time a galaxy is asymmetric due to a “flyby” encounter and the time for the galaxy to relax after the merger occurs. We therefore divide the CAS merger timescale into two different components: a flyby asymmetry time ($\tau_{\text{fly},A}$) and an asymmetry relaxation time ($\tau_{\text{relax},A}$). Note that these two quantities are solely defined as the time when the asymmetry value (A) is >0.35 . In the simulations we analyze, the merger begins to relax after 0.7 Gyr, which we use as the dividing line between the flyby and relaxation timescales. If there is more than one flyby before the final merger, then the timescale will include several factors of $\tau_{\text{fly},A}$. We denote the number of flyby interactions as N_{fly} and express the merger asymmetry timescale ($\tau_{\text{merger},A}$) as

$$\tau_{\text{merger},A} = (N_{\text{fly}}) (\tau_{\text{fly},A}) + (\tau_{\text{relax},A}). \quad (9)$$

To calculate merger rates using $\tau_{\text{merger},A}$, we use the average results of the major merger simulations where the fainter member of the pair under study was not removed, namely, τ_2 (Table 1), with a total asymmetry merger timescale of 0.43 ± 0.08 . This is the simulation in which the analysis mode matches the method used to derive the merger fractions in the Hubble Deep Fields. We find on average that the flyby timescale is $\tau_{\text{fly},A} \sim 0.23 \pm 0.05$ Gyr, which we find is relatively independent of mass ratio. Because this time is due to dynamical friction, it is also relatively independent of total mass (Carlberg et al. 2000). We further find from the τ_2 simulations that the average relaxation timescale is $\tau_{\text{relax},A} = 0.20 \pm 0.05$ Gyr, which is also largely independent of the merger mass ratio. The small error range on these numbers results from using sim2 from Table 1, whose total asymmetry time range is 0.08 Gyr (§ 3.3). This is likely an underestimate, as the actual range in physical properties is certainly larger than

what current N -body simulations can provide. Later, we add uncertainties from the merger fractions, and the 0.1 Gyr uncertainty due to the viewing angle, to these errors when computing merger rates and the merger history (§ 4).

From equation (8), the value of $\tau_{\text{relax},A}$ also depends slightly on the mass of the merger remnant. As the total mass of our simulated galaxies is $3.25 \times 10^{11} M_{\odot}$, we can write the asymmetry merger timescale as a function of mass (M_{tot}) as

$$\begin{aligned} \tau_m &= \tau_{\text{merger},A} \\ &= (0.23 \pm 0.05) N_{\text{fly}} + (0.15 \pm 0.05) \left(\frac{M_{\text{tot}}}{10^{11} M_{\odot}} \right)^{1/4}. \end{aligned} \quad (10)$$

We use equation (10) for the asymmetry merger timescale in the following calculations. For the reasons discussed in § 3.3.3 we only consider cases when $N_{\text{fly}} = 1$. There are two other systematic errors that we also consider. First, there is a possible systematic increase in the merger timescale of +0.35 Gyr if the galaxies undergoing mergers do not include a bulge. Observations suggest that the most massive galaxies at $z \sim 2.5$ have a central light concentration, often consistent with bulgelike features (Conselice et al. 2005b; Ravindranath et al. 2005); thus, it is not likely that many of the massive galaxies merging at this time are pure disks. Simulations also suggest that modern ellipticals formed from bulgelike systems, as pure disk mergers do not produce correct elliptical galaxy scaling relationships (Gonzalez-Garcia & Balcells 2005). The timescale given by equation (10) is also similar to that found empirically for real disk-disk mergers (Hernandez-Toledo et al. 2005).

We can then derive from equation (10) the rate of galaxy merging for systems with different masses and luminosities (Fig. 5). To calculate merger rates we use equations (6) and (10), where for a Milky Way mass galaxy, $\tau_m = 0.43$ Gyr. We use in equation (6) the best-fit merger fraction values as a function of redshift, $f_{\text{gm}}(z)$, as discussed in § 3.1. We assume $M_{\text{tot}}/M_* = 10$ and $M_*/L_B = 5$ to convert luminosities and stellar masses into total masses. The number densities of galaxies at various redshifts used in equation (6) are computed using the observed total number of galaxies in these various calculations (Conselice et al. 2003a, 2003b; Patton et al. 2000, 2002). Finally, Figure 5 shows the calculated merger rates in comoving volume units and in physical volume units.

Figure 5 shows that the merger rate at all luminosities and masses is relatively constant from $z \sim 3$ to $z \sim 1$, but drops rapidly at $z < 1$. This implies that from $z \sim 3$ to $z \sim 1$ galaxy mergers are very common, but at later times they drop quickly. This can be seen directly in the galaxy population. The gross morphologies of galaxies at $z \sim 1$ are very similar to their distributions and properties at $z \sim 0$ (Conselice et al. 2005a). This would not be the case if major mergers were still occurring in large numbers, as spiral galaxies would rapidly evolve morphologically as they merge (e.g., Hernandez-Toledo et al. 2005).

Furthermore, Figure 5 shows that the merger rate is high for lower mass and fainter galaxies, such that there are more major mergers occurring per unit time, per unit volume, than for the most massive systems. However, because there are so many low-mass and faint galaxies at all redshifts, the merger fraction is lower than for massive and luminous galaxies (Fig. 1; Conselice et al. 2003c). An important question to ask is why the merger fraction is so much lower for the lower mass and less luminous galaxies. One possibility is that because higher mass and more luminous galaxies cluster more strongly than the lower mass and

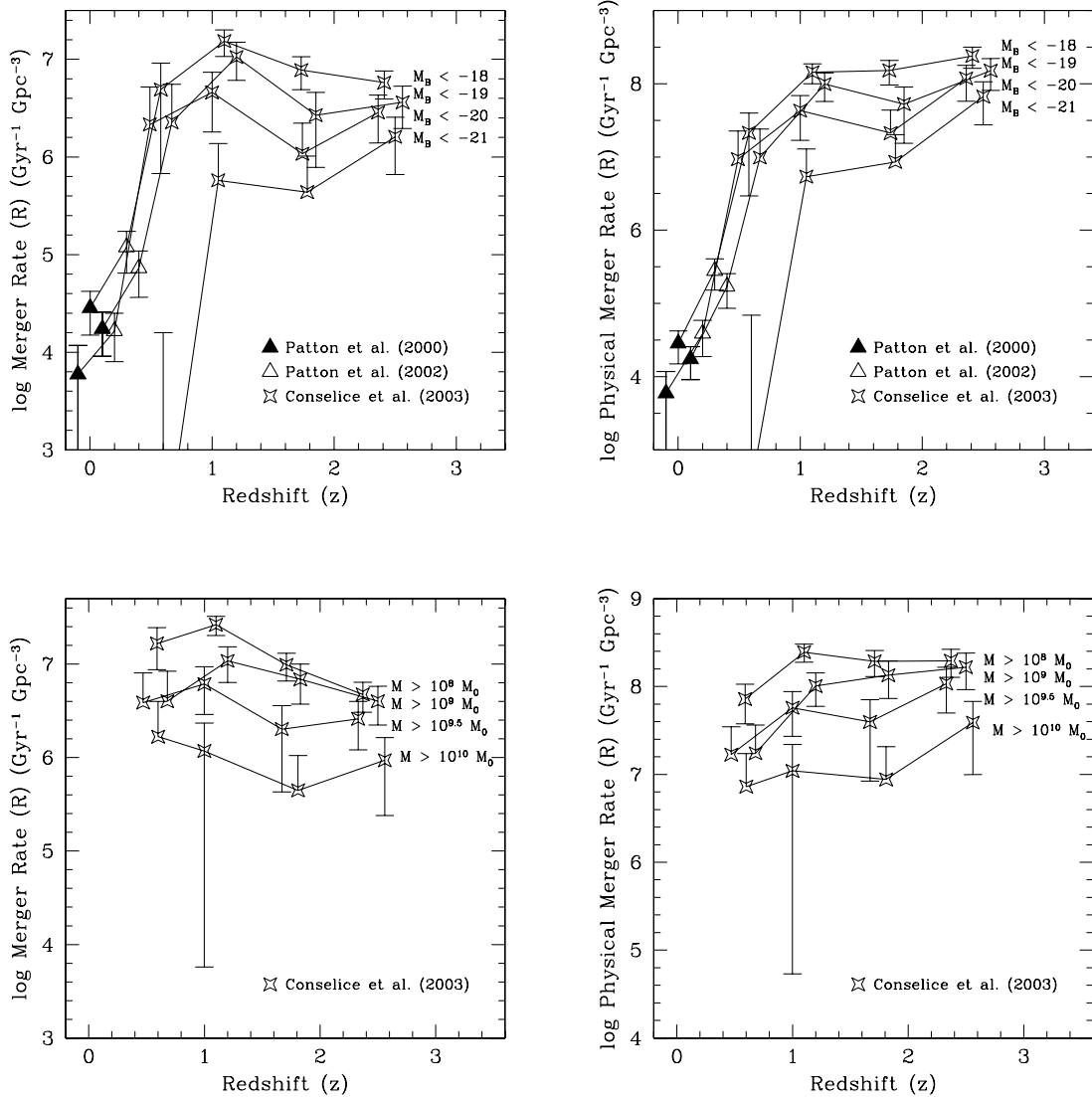


FIG. 5.—History of galaxy merger rates, in units of $\text{Gyr}^{-1} \text{Gpc}^3$, as a function of different initial masses and luminosities starting at $z \sim 3$. Plotted on the left is the merger rate within comoving volumes, while the right panels plot the merger rate within physical volumes. Plotted here are merger rates computed from the observed galaxy merger fractions in Conselice et al. (2003a) and Patton et al. (2002, 2000). Some points are shifted by ± 0.1 in redshift to allow individual points to be better seen. The error bars include uncertainties from the merger pair fractions as well as uncertainties from the merger timescales. Errors that are larger than their data point are shown by (accurate) one-sided upper error limits. The $M_B < -21$ point, below the $3 \text{ Gyr}^{-1} \text{Gpc}^{-3}$ plot limit on the comoving merger rate plot, has a value of $1.9 \text{ Gyr}^{-1} \text{Gpc}^{-3}$ at $z = 0.6$. Likewise, the similar point in the physical merger rate has a value of $2.5 \text{ Gyr}^{-1} \text{Gpc}^{-3}$ at $z = 0.6$.

lower luminosity systems (e.g., Giavalisco & Dickinson 2001; Adelberger et al. 2005), the most massive systems are more likely to merge. Minor mergers are likely playing some role in the formation of galaxies at the redshifts we study; however, we cannot place constraints on this process using the current techniques.

Another result from our simulations is that the CAS methodology for finding mergers can be successfully used to find major mergers. This means we can make reasonable assumptions about how much mass is added to galaxies identified as ongoing mergers. We hereafter assume that the average accreted galaxy pair is 65% of the mass of the original, or that the mass ratio of mergers is 1:1.5 in the calculations that follow.

4. MASSIVE GALAXY EVOLUTION DUE TO MERGERS

4.1. The Major Merger History of Massive Galaxies

Understanding the modes of star formation at high redshift, that is, determining what triggers the formation of stars, is still

largely uncertain. One of the first attempts to quantify this was in Conselice et al. (2003a, 2005b), where it was argued that a significant fraction of galaxies at high redshift are undergoing mergers. We further argued that the merger rate and mass accretion rate due to mergers can be computed using assumptions about the merger timescale at high redshift. Thus, using the results from the N -body simulations discussed above, we can now tentatively calculate the history of galaxy merging for the first time.

If we assume that $z < 3$ galaxies are undergoing major mergers in the quantitative way described earlier through the computed galaxy merger fractions, then we can use this characterization to determine the average number of major mergers an average galaxy of a given mass at $z \sim 3$ will undergo by the time it reaches $z \sim 0$. This is computed by integrating the merger rate divided by the density, or the fraction of galaxies observed at each redshift undergoing a major merger divided by the timescale in which a merger remains identifiable as a merger (τ_m). By

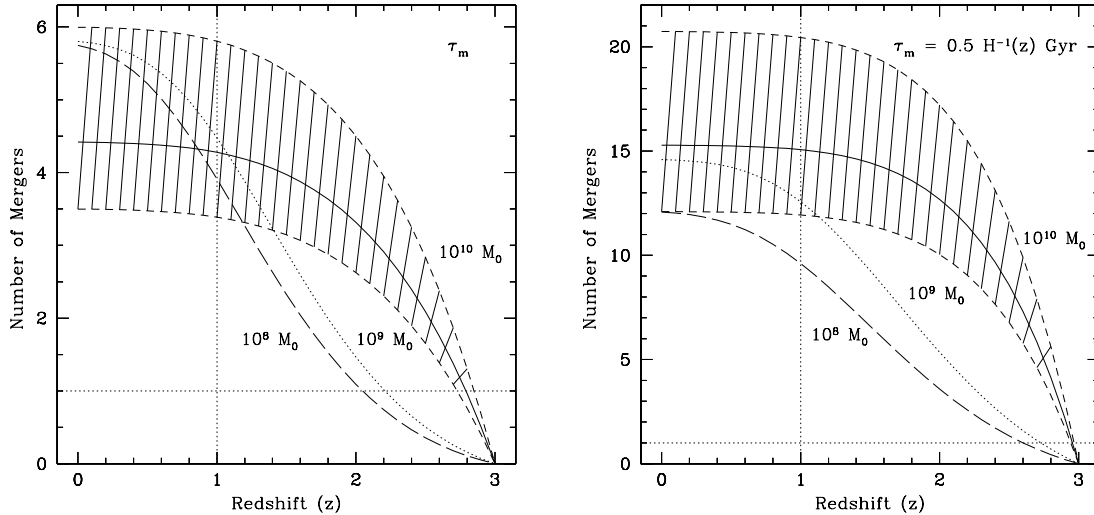


FIG. 6.—Cumulative number of major mergers (1:3 or lower mass ratios) for galaxies starting from $z = 3$ for systems with different initial stellar masses. The solid line shows the evolution in the cumulative number of mergers for an average galaxy with an initial mass of $10^{10} M_{\odot}$, with the hatched region showing the 1σ range of possible outcomes. This 1σ range includes uncertainties in the merger timescales as well as uncertainties in the measured merger fractions. For lower mass galaxies, the number of mergers is shown as the dashed line for systems with $M_* > 10^8 M_{\odot}$ and the dotted line for systems with $M_* > 10^9 M_{\odot}$.

integrating this, we obtain the number of mergers an average galaxy undergoes between z_1 and z_2 (N_m),

$$N_m = \int_{z_1}^{z_2} \frac{f_{\text{gm}}(z)}{\tau_m} dt = \int_{z_1}^{z_2} t_{\text{H}} \left(\frac{f_0}{\tau_m} \right) (1+z)^{m_A-1} \frac{dz}{E(z)}, \quad (11)$$

where f_{gm} is the galaxy merger fraction, τ_m is the asymmetry merger timescale (eq. [10]), and the parameter $E(z) = [\Omega_M(1+z)^3 + \Omega_k(1+z)^2 + \Omega_{\Lambda}]^{-1/2} = H^{-1}(z)$. We have assumed a power-law increase for the form of f_{gm} , since this is the best fitting formula for the most massive and most luminous galaxies. This is easy to change when considering power-law/exponential fits for lower mass galaxies, which we do when determining the number of mergers and the resulting mass accreted in these systems. This calculation also requires that we track the evolution of the stellar masses of these galaxies, as the values of m_A and f_0 evolve with time and stellar mass. However, for the most massive galaxies we do not have the mass resolution at $M_* > 10^{10} M_{\odot}$ to carry out this solution. Future studies that use larger samples will have this resolution, and a formal solution using equation (11) can be applied with the evolving merger history included.

According to this formalism, and using the best-fit values for m_A and f_0 , we calculate the merger history of galaxies at various initial masses and luminosities. Figure 6 shows the cumulative number of mergers an average galaxy with an initial stellar mass of 10^{10} , 10^9 , and $10^8 M_{\odot}$ undergoes as a function of redshift, starting at $z \sim 3$. Just as in § 3.3.4, we use the merger timescale from sim2 (Table 1) and include in the error budget the timescale range from different orbital properties, mass ratios, and viewing angles.

Based on this, we find that a $10^{10} M_{\odot}$ galaxy will experience $4.4^{+1.6}_{-0.9}$ major mergers according to this formalism by $z \sim 0$ using equations (10) and (11). If we consider that mergers occur with two flybys instead of the one we assume, then the total number of mergers will be ~ 3 , and if we assume that all of these mergers occur with pure disks as progenitors, then an average system will undergo ~ 3 mergers. However, as argued in § 3.3.3 and above, neither of these extreme scenarios is likely.

It is possible that the merger timescales for galaxies are shorter at higher redshifts than at $z \sim 0$, which would imply that the asym-

metry timescale τ_m would also be shorter. We use the observed evolution of the sizes of high-redshift galaxies to approximate how the merger timescale could possibly change as a function of redshift. Ferguson et al. (2004) find that the sizes of Lyman break galaxies evolve with redshift such that the average measured radius increases as $H^{-1}(z) = E(z) = [0.3(1+z)^3 + 0.7]^{-1/2}$ in our cosmology. If the merger timescales increase linearly with radius, then $\tau_m(z) \sim E(z)$. When we consider this evolution of τ with redshift, we find that the most massive galaxies undergo more mergers between $z = 3$ and 0, roughly $15.2^{+5.4}_{-3.2}$. We also calculate these curves for the lower mass galaxies using the power-law/exponential formalism for the merger fraction history f_{gm} in equation (11). This is, however, an extreme scenario, and there is no evidence that the merger timescale at high redshift is any shorter than it is at $z \sim 0$.

Interestingly, in all cases the lower mass galaxies experience a similar number of mergers by $z \sim 0$ (Fig. 6). The major difference is that for the most massive galaxies, most of these mergers occur earlier at $z > 1$, while the lower mass systems have few major mergers at similar redshifts. Most merging for galaxies with $M > 10^{10} M_{\odot}$ appears to be complete by $z \sim 1.5$, with no major mergers after this time. This implies that massive galaxy formation is complete by $z \sim 1.5$, if major mergers are the dominant mechanism for forming high-mass systems.

4.2. Stellar Mass Evolution of Field Galaxies

The stellar mass of a galaxy undergoing a merger increases due to the stellar mass accreted in the merger, as well as from any star formation induced during the merger. Below we present a very general calculation and formalism for calculating the way stellar mass can be increased in galaxies during the merger process. Since galaxies at high redshift are thought to be gas-rich systems, the amount of stars produced during a burst can be quite significant. There are some estimates for the ongoing and past star formation rates in Lyman break galaxies that we use to determine how much stellar mass is added due to the star formation induced during a merger. In general, the total amount of stellar mass added to a galaxy over time is given by δM_T ,

$$\delta M_T = \delta M_{\text{msf}} + \delta M_{\text{asf}} + \delta M_{\text{merger}},$$

where δM_{msf} and δM_{asf} are the amounts of stellar mass added due to star formation induced by the merger and from gas accretion, respectively, while δM_{merger} is the amount of stellar mass added due to the merger process. Since from § 3.3 we know that only mergers with mass ratios of 1:3 or less will produce the signal for a major merger in the CAS system, the amount of mass added in a merger detected through the CAS method must be similar to the original galaxy's mass.

The amount of stellar mass added due to star formation induced from a merger can be calculated from fitting the spectral energy distributions (SEDs) of high-redshift star-forming galaxies to model star formation histories. By doing this, the best form for the star formation history can be retrieved. Several studies have investigated the stellar populations, star formation history, and stellar masses of galaxies at $z \sim 2-3$. What is generally found is that the star formation history can be fitted as either constant, exponential, or in bursts, but the exponential model gives the most general and best fit (Papovich et al. 2001).

In Papovich et al. (2001) and Shapley et al. (2001), the spectral energy distributions of LBGs are fitted to a star formation model that gives the current star formation rate (Ψ), the e -folding time of the starburst (τ_{sf}), and the current stellar mass at solar and 0.2 solar metallicities, and with Salpeter and Scalo initial mass functions (Shapley et al. 2001 only fitted for solar metallicity, however). These models generally assume that the star formation history exponentially declines from an initial star formation rate Ψ_0 , such that the star formation rate at a given later time t is

$$\Psi(t) = \Psi_0 \exp(-t/\tau_{\text{sf}}). \quad (12)$$

This fitting also gives an age for the burst (t_{sf}). This is, however, the star formation law for the most recent burst of star formation. If there are several episodes of star formation, this is not easily revealed through the SEDs of galaxies. One problem with these fits is that they are based only on SEDs out to the observed K band, and thus could in principle be missing a significant amount of older stellar mass. Preliminary results using *Spitzer* observations reveal that there is not a large missing old stellar population in Lyman break galaxies, and the fitted Ψ_0 and τ_{sf} parameters do not differ significantly after adding in the rest-frame near-infrared to the SED fitting (Barmby et al. 2004).

We perform calculations of how much stellar mass is added to galaxies due to induced star formation with some trepidation, since the exact form of the star formation history of galaxies is still largely undetermined from observations and may not have a unique solution or standard form. The following results should be taken as a general first step at solving this problem, and not as a final quantitative result.

Although the starbursts we see in LBGs are ongoing, and thus have already created some of their stellar material, we use these fits to predict how much stellar mass will be created through future events by assuming future star formation will be similar and induced during each merger. The amount of stellar mass created through starbursts induced through mergers (δM_{msf}) is then

$$\delta M_{\text{msf}} = \int_{z_1}^{z_2} \int_0^{t_m} t_{\text{H}} \left(\frac{f_0}{\tau_m} \right) (1+z)^{m_A-1} \frac{dz}{E(z)} \Psi_0 \exp\left(-\frac{t}{\tau_{\text{sf}}}\right) dt, \quad (13)$$

where z_2 and z_1 are the final and observed redshifts, respectively, t_{H} is the Hubble time, and t_m is the time from the onset of the merger until the present day, and for integration purposes can be effectively considered infinite. When $t_m \gg \tau_{\text{sf}}$, we can approximate the star formation part of equation (13) as $\Psi_0 \tau_{\text{sf}}$. We can

then compute the amount of stellar mass added during mergers due to induced star formation as $\delta M_{\text{msf}} = \Psi_0 \tau_{\text{sf}} N_m$, where N_m is the number of major mergers. For these calculations we use the median values, $\tau_{\text{msf}} = 20$ Myr and an ongoing star formation rate $\Psi_0 = 32 M_\odot \text{ yr}^{-1}$, for $z > 2$ LBGs (Papovich et al. 2001). We normalized the initial star formation rate by computing the average specific star formation rate for the Papovich et al. sample and calculated the actual star formation rate for each galaxy mass by assuming that the specific star formation rate is scale free. We obtain very similar results if we use the average star formation rate for all stellar masses. We also include the amount of stellar mass added from the ongoing merger (δM_{asf}) observed in each system through a similar method. There are some caveats to this approach. The first is that the values of τ_{msf} in Papovich et al. are not well constrained. As such, it is possible that our reconstructed star formation histories are not representative of the actual stellar mass produced in high-redshift star formation events. An alternative method is to assume that the star formation is produced in bursts within a given duration at a constant rate. The implementation of this formalism results in effectively the same mass formed as the exponential star formation rate over an infinite (or very long) period of time. If the burst duration is 100 Myr, then the amount of mass formed would be roughly 3 times higher than the exponential star formation decline.

To obtain the stellar mass added to a given galaxy through the mergers themselves, we tried two methods, which are nearly identical. First, we used the empirical formalism in Conselice et al. (2003a), which gives the amount of stellar mass accretion onto a galaxy due to major mergers as a function of redshift. This can be generalized as

$$\delta M_{\text{merger}} = \int_{z_1}^{z_2} \frac{1}{f_0} (1+z)^{m_A} \frac{\Delta M}{\tau_m} (1+z)^{m_M} dt, \quad (14)$$

where dt , as before, is given by $dt = t_{\text{H}} dz / [(1+z)E(z)]$, and $\Delta M(1+z)^{m_M}$ is the empirically calculated stellar mass added to a galaxy due to major mergers every Gyr per galaxy. We also estimated the number of mergers a galaxy undergoes using the relationship $\delta M_{\text{merger}} \sim 2^{N_m} M_0$ for equal mass mergers, or in our case $1.65^{N_m} M_0$ for 1:1.5 mass ratio mergers, where M_0 is the initial stellar mass of the galaxy. Both methods give similar stellar mass accretion rates from the major merger process.

By using τ_m from equation (10), and the values $m_A = 2.7 \pm 0.5$, $f_0 = 0.01$, and $m_M = 1.47$, based on our empirical fits discussed in this paper for galaxies with $M_* > 10^{10} M_\odot$, we compute the final $z \sim 0$ stellar mass of an average massive ($M_* > 10^{10} M_\odot$) $z = 3$ galaxy. The result of these calculations is shown in Figure 7, where the stellar mass buildups for galaxies of different initial stellar masses are shown. Based on this, it can be seen that the most massive galaxies, those with $M_* > 10^{10} M_\odot$ at $z \sim 3$, appear to evolve into galaxies with stellar masses $\sim 10^{11} - 10^{12} M_\odot$ by $z \sim 0$. Thus, from the merger process, Lyman break galaxies can become the most massive galaxies in today's universe. The lower stellar mass systems, with $M_* > 10^9 M_\odot$ and $M_* > 10^8 M_\odot$, also increase by up to 2 orders of magnitude in stellar mass due to the major merger process (Fig. 7).

The majority of this increase in stellar mass is due to the major merging activity. That is, their stellar mass increases over time because there are on average 4–6 major mergers occurring per galaxy, and each one will slightly less than double the stellar mass. The star formation appears to contribute a small fraction, roughly 10%–30% of the new mass, although this can be much higher (up to 50%) if we consider a larger amount of star formation within bursts, as discussed above.

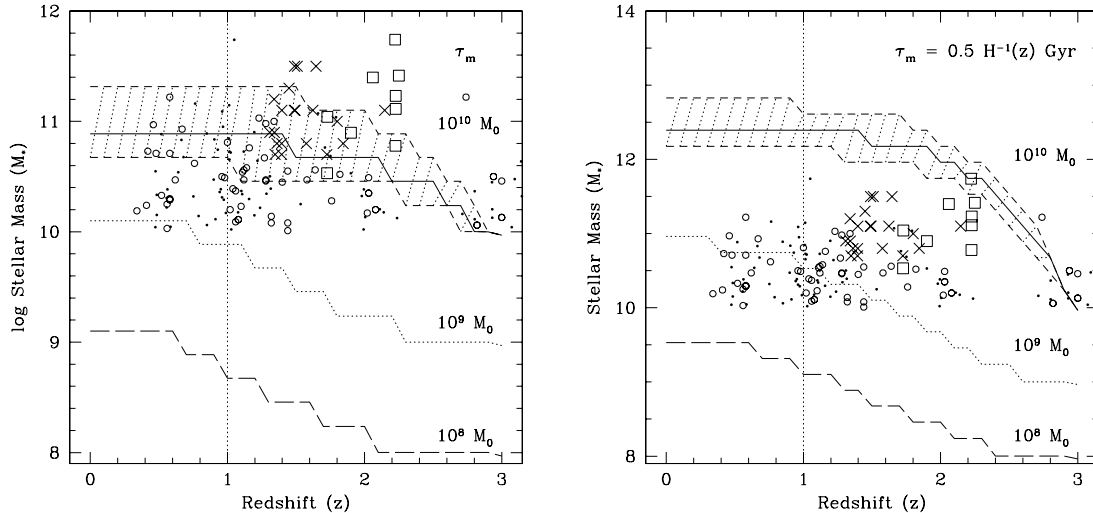


FIG. 7.—Average evolution of stellar masses for galaxies with various initial stellar masses, starting at $M_* = 10^{10}$, 10^9 , and $10^8 M_\odot$. The vertical dotted line is $z \sim 1$. The range of possible final stellar masses using the observed merger fraction evolution, and the amount of induced stellar mass, is shown in the shaded region. Also plotted are observed stellar masses for galaxies from the HDF-N (Dickinson et al. 2003; *dots*), HDF-S (Franx et al. 2003; Conselice et al. 2005b; *open circles*), K20 survey (Daddi et al. 2004; *boxes*), and the Gemini Deep Deep Survey (McCarthy et al. 2004; *crosses*).

In summary, it appears that the most massive LBGs at $z \sim 3$ can become galaxies with stellar masses $\sim 10^{12} M_\odot$. These galaxies rapidly merge between $z \sim 3$ and $z \sim 2$, where the mass increases by a factor of 10. We find that there are no mergers, and thus no addition of stellar mass due to the major merger process at $z < 1.5$, for these systems. We see a slightly different pattern for the lower mass systems with $M_* > 10^9 M_\odot$ and $M_* > 10^8 M_\odot$. Figure 6 shows that there is not as much merger activity for the lower mass systems between $z \sim 2$ and $z \sim 3$. There is, however, a similar number, if not more mergers, at lower redshifts. In fact, most of the merging activity at lower redshift occurs for these lower mass galaxies, consistent with direct mass determinations of galaxies that are merging at $z < 1$ (Bundy et al. 2005).

5. DISCUSSION

5.1. Possible Objections to the Merger Scenario

We find that massive Lyman break galaxies at $z \sim 3$ will undergo 4–6 major mergers from $z \sim 3$ until $z \sim 0.5$, with most occurring between $z = 2$ and 3. Lower mass systems have a merger history whereby more mergers occur at lower redshifts, although these systems also gain up to 100 times their initial mass through the merger process.

There are several possible objections to this picture, including the number counts of galaxies at different redshifts and the observed age of starbursts in $z > 2$ galaxies. The first requires that the comoving number densities of evolved massive LBGs match the number density of $z \sim 0$ massive systems. Since the density of LBGs roughly matches the density of massive spheroids today (Steidel et al. 1996), we cannot destroy or create too many new massive galaxies through mergers. There must be a balance such that as LBGs effectively disappear through mergers, there must be fainter and lower mass systems to replace them. For the most massive galaxies, this effectively requires in general that the number of massive galaxies,

$$\begin{aligned}
 N(M_* > 10^{10} M_\odot)(z - \delta z) &= N_{\text{tot}}(M_* > 10^{10} M_\odot)(z) \\
 &\quad - f_{\text{gm}}(z)N_{\text{tot}}(M_* > 10^{10} M_\odot)(z) \\
 &\quad + f'_{\text{gm}}(z)N_{\text{tot}}(M_* > 10^{10-\delta} M_\odot)(z),
 \end{aligned}$$

remain constant at redshifts $z < 3$, where δ is small (< 1). This requires that $f_{\text{gm}}N_{\text{tot}}(M_* > 10^{10} M_\odot) = f'_{\text{gm}}N_{\text{tot}}(M_* > 10^{10-\delta} M_\odot)$ at all redshifts, or $f_{\text{gm}}/f'_{\text{gm}} = N_{\text{tot}}(M_* > 10^{10-\delta} M_\odot)/N_{\text{tot}}(M_* > 10^{10} M_\odot)$. The value of $f_{\text{gm}}/f'_{\text{gm}} \sim 5$ at $z > 2$, using the $10^{9.5} M_\odot$ value for f'_{gm} . This is similar to $N_{\text{tot}}(M_* > 10^{9.5} M_\odot)/N_{\text{tot}}(M_* > 10^{10} M_\odot)$ at the same redshift. Based on this, it appears that the number densities of the most massive galaxies will remain roughly the same as the observed densities of LBGs, which are similar to the densities of modern massive galaxies. This result originates from the fact that while there is a higher merger fraction for the more massive galaxies, there are more lower mass galaxies undergoing mergers at all redshifts (Fig. 5).

A related issue is the stellar mass to dark matter ratio of Lyman break galaxies. Although this ratio is not known for certain, there are indications that the Lyman break galaxies are associated with the most massive halos of today (Adelberger et al. 1998), while stellar masses for the most massive systems are typically around $10^{10} M_\odot$. If mergers were the dominant source of the buildup of galaxies from LBGs without any star formation, the ratio of stellar to total mass would remain constant. If the halo masses of LBGs are of the order of $10^{12} M_\odot$, then there must be further star formation to match the ratio of stellar to halo masses of 0.1 found today and even by $z \sim 1$ (Conselice et al. 2005b). Although we find that up to 30% of the additional mass is formed in star formation, the majority originates from the existing mass in the mergers. It is also not certain that LBGs have a stellar to total mass ratio of 0.01. Often, the total masses of $z > 2$ galaxies are less than their stellar masses (Shapley et al. 2004), making the total or stellar (but likely total) masses suspect. Furthermore, the halo occupation number for LBG halos may be larger than 1, such that there is more than one galaxy in a single massive halo. This indeed seems to be the case based on recent measurements of the LBG correlation function that show that there is an excess at small scales (Lee et al. 2006), possibly the result of ongoing mergers and multiple galaxies in single halos.

Another possible objection is that the ages of the stellar populations in LBGs are too old at $z > 2$ to be produced in bursts induced by the large number of mergers occurring between $z \sim 2$ and $z \sim 3$. In other words, the observed ages of some starbursts between $z \sim 2$ and $z \sim 3$ are longer than the elapsed time between

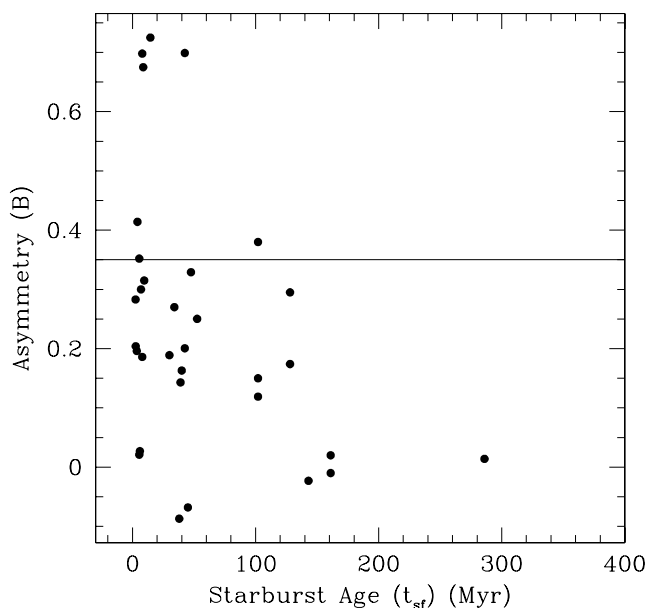


FIG. 8.—Relationship between the age of the most recent starburst for galaxies at $z > 2$, as a function of rest-frame B -band asymmetry values. These ages are taken from Papovich et al. (2001) using the 0.2 solar and Salpeter IMF models. The systems with asymmetries consistent with undergoing a merger are above the solid line. These systems typically have younger starburst ages. This implies that the asymmetry index is a good indicator for recent mergers, as all of these systems have ages < 100 Myr.

$z \sim 2$ and $z \sim 3$, and thus it would be difficult to have several mergers and accompanying star formation occur during this time. Papovich et al. (2001) and Shapley et al. (2001) have found a wide range of stellar population or burst ages for galaxies within this redshift range. Some of these ages are as old as 1 Gyr. Clearly not all LBGs are involved in the multiple mergers discussed here, unless these time estimates are incorrect. There is some evidence for this, as the age of the starburst can vary by many factors depending on the choice of initial mass function (IMF) and metallicity (Papovich et al. 2001). However, there are reasons to believe that these “older” bursts are occurring in the lower mass systems (Shapley et al. 2001), which are also the more symmetric systems (Conselice et al. 2003a, 2003b).

In general, however, it appears that many of the best-fit starburst ages for LBGs are short < 100 Myr, particularly when a metallicity of 0.2 solar is used (Papovich et al. 2001). In fact, the systems identified in Conselice et al. (2003a), and in this paper, as mergers have young starburst ages, consistent with interpreting their star formation as produced in a recent merger event. This correlation can be seen in Figure 8, which plots the ages of the most recent starburst and the asymmetries of their galaxies for $z > 2$ LBGs (Papovich et al. 2001). The galaxies with high asymmetries, $A > 0.35$, and thus likely merging (above the solid line), all have young ages, typically less than 50 Myr. These merging systems also have the highest ongoing star formation rates. Since N -body models show that not all phases of a merger have a high asymmetry, it is possible that the symmetric young-age LBGs are in a phase of a merger in which they are not asymmetric.

5.2. Implications for Massive Galaxy Formation

If the merger history at $z > 1$ as derived in Conselice et al. (2003a) and used in this paper to calculate the formation history of galaxies holds up with future observations and techniques, it has profound implications. It implies that we have observationally solved how and when most massive galaxies formed.

Our results are qualitatively consistent with several other apparently paradoxical results, a number of which have questioned the foundation of the modern theoretical galaxy formation paradigm, cold dark matter.

Recently, various groups have discovered massive galaxies at redshifts $z > 1$, which has been seen as potentially a problem for CDM-based models (Franx et al. 2003; Daddi et al. 2004; Somerville et al. 2004; Glazebrook et al. 2004; cf. Nagamine et al. 2005). For example, Glazebrook et al. (2004) find that the stellar mass density of massive galaxies, with $M_* > 10^{10.8} M_\odot$, is roughly an order of magnitude larger than expectations based on a semianalytic CDM model of galaxy formation (Cole et al. 2000; Benson et al. 2002), although the agreement with the $M_* > 10^{10.2} M_\odot$ models is quite good. This implies that the most massive galaxies formed earlier than what CDM models predict. There are two possible solutions to this. The first, presented in this paper, is that the merger rate, and the fraction of galaxies at high redshift that are merging, is higher than what is predicted in CDM models.

This mismatch with CDM models can be seen through the comparison in Figure 1. Figure 1 shows that this particular CDM model, from semianalytic galaxy formation modeling (Benson et al. 2002), generally underpredicts the merger fraction we observe, as do other semianalytic model predictions (Somerville et al. 2001). This suggests that the solution to the “massive galaxies at high redshift problem” is not a rapid collapse with no mergers, but that there are possibly *more* mergers at higher redshift than what semianalytic CDM models predict. Our results suggest that massive galaxies should be well formed by $z \sim 1.5$, which is consistent with observations of galaxy stellar masses (Fig. 7). An alternative scenario is that these studies are biased by cosmic variance. It is possible that the Glazebrook et al. (2004) and Franx et al. (2003) studies are examining overdense regions at their particular redshifts. Wider area infrared surveys are clearly needed to make progress in understanding this issue.

An early formation history for massive early-type galaxies explains a number of other observations. The first is that the morphological distribution of galaxies on the Hubble sequence is largely in place by $z \sim 1$ (Conselice et al. 2005b), with a similar number density of disk galaxies as today (Ravindranath et al. 2004). Another is that the clustering properties of massive galaxies appear to be largely in place by $z \sim 1$ (Coil et al. 2004), as is the size distribution (Ferguson et al. 2004), with galaxy sizes growing between $2 < z < 6$ (Bouwens et al. 2004). The metallicities of massive galaxies at $z > 2$ are also similar to the most massive galaxies found today, with values of solar or greater (Shapley et al. 2004; van Dokkum et al. 2004), suggesting that there are not many future generations of massive starbursts. Another observation consistent with a rapid and early merging history for massive galaxies is that the number of metal-poor globular clusters around early-type galaxies correlates with galaxy luminosity (Strader et al. 2004), implying that their formation occurred at $z > 2$. This does not, however, relieve other problems with the hierarchical formation of galaxies, as there are massive systems well formed by $z \sim 6$ in the form of QSOs that contain high metallicities (Barth et al. 2003) that might also contain massive galaxies. Clearly, probing the merging history at $z > 3$ will be insightful.

Major mergers at $z < 3$ also relate to the buildup of black holes at similar redshifts. The peak of the merger rate and merger fraction coincides with the peak of active galactic nucleus (AGN) and QSO activity. Thus, it seems likely that the buildup of black holes and galaxy bulges, which is already present in some form at

$z \sim 1$ (Grogin et al. 2005), could be driven by the major merger process. As there is little correlation between the presence of merging activity and X-ray flux for LBGs (Lehmer et al. 2005), this implies that there is some delay between the formation of black holes and the merger.

One problem that we have not addressed is the fact that only $\sim 10\%$ – 20% of all stellar mass is formed by $z \sim 3$ (Dickinson et al. 2003; Rudnick et al. 2003), and thus there must be, and is, significant star formation at $z < 3$ (Giavalisco et al. 2004b). Since only 10% – 30% of the stars in a massive galaxy form by starbursts induced in major mergers, there must be other methods of forming new stars at $z < 3$. At lower redshifts, when the merger rate declines, other methods such as dissipation to form disks at $1 < z < 2$, or secular evolution produced by bars, which are common at $z \sim 1$ (Jogee et al. 2004), must dominate the stellar mass assembly. Since spheroids dominate the stellar mass density of nearby galaxies, containing roughly a third to half of all stars (Tasca & White 2005), it is not likely that all this mass is produced in major mergers. It appears that the lower mass spheroids are produced through dissipative processes at $z < 1$, when they are found to be bluer systems (Stanford et al. 2004), while the higher mass systems, which are generally in denser environments, are produced through major mergers at earlier times.

We have also not discussed the relationship between the submillimeter-bright galaxies found at $z > 1$ and the systems studied in this paper. The Lyman break galaxies we examined are much more common at high redshift than submillimeter sources, yet the relationship between submillimeter sources and Lyman break galaxies is still largely unknown. It is possible that the submillimeter sources are the most massive galaxies at high redshift, as suggested by their clustering properties (Blain et al. 2004). In any case, the morphologies of the limited number of submillimeter sources that have been studied show that these systems are large galaxies that are undergoing major mergers (Conselice et al. 2003b; Chapman et al. 2003; Pope et al. 2005), with preliminary indications that the submillimeter sources are involved in a more active phase of a merger than the most massive LBGs studied in the Hubble Deep Field (Conselice et al. 2003c).

6. SUMMARY

In the first part of this paper we reduce all known merger fractions to a common scale based on the fraction of *galaxies* undergoing a merger at a given redshift, and within a range of stellar mass or luminosity. We then show that the best fitting function for the galaxy merger fraction history is a combined power/exponential formalism for systems with $M_* < 10^{10} M_\odot$ and $M_B > -20$ out to $z \sim 3$. For the brightest and most massive systems with $M_B < -20$ and $M_* > 10^{10} M_\odot$ out to $z \sim 3$, and for lower mass and fainter systems out to $z \sim 1$, a simple power law is suitable for describing the redshift dependence of the merger fraction.

We then analyze a suite of self-consistent major and minor merger N -body simulations with the CAS structural analysis system. We find that major mergers, defined as having a mass ratio of 1:3 or lower, always produce asymmetric systems, typically for 300 Myr, independent of viewing angle or relative orbital configuration of the pair, with a slight dependence on mass, which we

account for. We investigate in detail the structure of a 1:5 merger and find that during the 4 Gyr duration of this merger, the asymmetry parameter never becomes high enough to be identified as a merger in the CAS system. We then use this information to derive the galaxy merger rate. From this we calculate that an average massive galaxy, with $M_* > 10^{10} M_\odot$, undergoes $4.4^{+1.6}_{-0.9}$ major mergers using our derived merger timescale that slightly depends on mass (eq. [10]). Nearly all of this merging occurs by $z \sim 1.5$, after which an average massive galaxy experiences no further major mergers.

We then calculate how galaxies of various initial masses at $z \sim 3$ formed through major mergers. Our conclusion is that mass accreted during the major merger process, and the stars created from star formation induced by these mergers, is such that when these systems evolve to $z \sim 0$ they will be as massive as most galaxies in the modern universe. We calculate that a typical galaxy increases in mass by a factor of ~ 10 – 100 from this process. Our calculations are based on empirically determined merger fractions and rates from Conselice et al. (2003a) and include star formation scenarios based on observations of star formation histories of Lyman break galaxies. We calculate that 10% – 30% of the new stellar mass is formed in starbursts induced by these mergers, and the remainder comes from the merger itself. The merger scenario described in this paper naturally explains observations of massive and extremely red galaxies at $z > 1$, the distributions of modern elliptical galaxy ages, and metallicities, among many other massive galaxy properties.

Future results will expand our conclusions using better models and deeper *HST* observations. Wider area and deep infrared surveys at high resolution, either with WFC3 on *HST*, with *James Webb Space Telescope (JWST)*, and/or with ground-based adaptive optics, are needed to determine with certainty the merger rate at high redshift. Advanced Camera for Surveys (ACS) imaging of the Great Observatories Origins Deep Survey (GOODS) fields (Giavalisco et al. 2004a) will potentially allow us to make these determinations, although high-resolution deep infrared imaging is needed to make definitive progress.

The idea for this paper was initiated by a question from Harry Ferguson. However, as Jim Gunn says, “Partial answers are the only answers” (Morgan 1988), and unfortunately this work is no exception. I hope, at the very least, that this presentation begins a serious discussion of determining observationally *how* galaxies formed. I thank Chris Mihos for the use of his models and his critically important contributions to this paper, and for being a true gentleman. This work has furthermore benefited from collaborations and conversations with Matt Bershady, Kevin Bundy, Mark Dickinson, Richard Ellis, Jay Gallagher, and Casey Papovich. I furthermore thank Xavier Hernandez and James Taylor for illuminating discussions, Kevin Bundy and Russel White for helpful proofreads, Andrew Benson for the Galform models used in this paper, and finally the referee for making several important points. Support for this research was provided by NSF Astronomy and Astrophysics Postdoctoral Fellowship 0201656.

REFERENCES

- Aceves, H., & Velazquez, H. 2005, *MNRAS*, 360, L50
 Adami, C., et al. 2005, *A&A*, 429, 39
 Adelberger, K. L., Steidel, C. C., Giavalisco, M., Dickinson, M., Pettini, M., & Kellogg, M. 1998, *ApJ*, 505, 18
 Adelberger, K. L., Steidel, C. C., Pettini, M., Shapley, A., Reddy, N. A., & Erb, D. K. 2005, *ApJ*, 619, 697
 Allam, S. S., et al. 2004, *AJ*, 127, 1883
 Barmby, P., et al. 2004, *ApJS*, 154, 97
 Barth, A. J., Martini, P., Nelson, C. H., & Ho, L. C. 2003, *ApJ*, 594, L95
 Baugh, C. M., Cole, S., & Frenk, C. S. 1996, *MNRAS*, 283, 1361
 Benson, A. J., Lacey, C. G., Baugh, C. M., Cole, S., & Frenk, C. S. 2002, *MNRAS*, 333, 156

- Bernardi, M., et al. 2003, *AJ*, 125, 1866
- Bershady, M. A., Jangren, J. A., & Conselice, C. J. 2000, *AJ*, 119, 2645
- Blain, A. W., Chapman, S. C., Smail, I., & Ivison, R. 2004, *ApJ*, 611, 725
- Blain, A. W., Smail, I., Ivison, R. J., Kneib, J.-P., & Frayer, D. T. 2002, *Phys. Rep.*, 369, 111
- Bond, J. R., Cole, S., Efstathiou, G., & Kaiser, N. 1991, *ApJ*, 379, 440
- Bouwens, R. J., Illingworth, G. D., Blakeslee, J. P., Broadhurst, T. J., & Franx, M. 2004, *ApJ*, 611, L1
- Bower, R. G. 1991, *MNRAS*, 248, 332
- Boylan-Kolchin, M., Ma, C.-P., & Quataert, E. 2005, *MNRAS*, 362, 184
- Bundy, K., Ellis, R. S., & Conselice, C. J. 2005, *ApJ*, 625, 621
- Bundy, K., Fukugita, R. S., Ellis, R. S., Kodama, T., & Conselice, C. J. 2004, *ApJ*, 601, L123
- Capelato, H. V., de Carvalho, R. R., & Carlberg, R. G. 1995, *ApJ*, 451, 525
- Carlberg, R. G. 1990, *ApJ*, 350, 505
- . 1991, *ApJ*, 375, 429
- Carlberg, R. G., Pritchett, C. J., & Infante, L. 1994, *ApJ*, 435, 540
- Carlberg, R. G., et al. 2000, *ApJ*, 532, L1
- Chapman, S. C., Windhorst, R., Odewahn, S., Yan, H., & Conselice, C. 2003, *ApJ*, 599, 92
- Coil, A., et al. 2004, *ApJ*, 609, 525
- Cole, S., Lacey, C. G., Baugh, C. M., & Frenk, C. S. 2000, *MNRAS*, 319, 168
- Conselice, C. J. 1997, *PASP*, 109, 1251
- . 2002, *ApJ*, 573, 5L
- . 2003a, *ApJS*, 147, 1
- . 2003b, in *Galaxy Dynamics*, ed. C. Boily et al. (Les Ulis Cedex: EAS), 101
- Conselice, C. J., Bershady, M. A., Dickinson, M., & Papovich, C. 2003a, *AJ*, 126, 1183
- Conselice, C. J., Bershady, M. A., & Gallagher, J. S. 2000a, *A&A*, 354, L21
- Conselice, C. J., Bershady, M. A., & Jangren, A. 2000b, *ApJ*, 529, 886
- Conselice, C. J., Blackburne, J., & Papovich, C. 2005a, *ApJ*, 620, 564
- Conselice, C. J., Bundy, K., Ellis, R., Brichmann, J., Vogt, N., & Phillips, A. 2005b, *ApJ*, 628, 160
- Conselice, C. J., Chapman, S. C., & Windhorst, R. A. 2003b, *ApJ*, 596, L5
- Conselice, C. J., & Gallagher, J. S. 1999, *AJ*, 117, 75
- Conselice, C. J., Gallagher, J. S., Calzetti, D., Homeier, N., & Kinney, A. 2000c, *AJ*, 119, 79
- Conselice, C. J., Gallagher, J. S., III, & Wyse, R. F. G. 2001, *AJ*, 122, 2281
- . 2002, *AJ*, 123, 2246
- . 2003c, *AJ*, 125, 66
- Conselice, C. J., et al. 2004, *ApJ*, 600, L139
- Daddi, E., et al. 2004, *ApJ*, 600, 127L
- Dickinson, M., Papovich, C., Ferguson, H. C., & Budavári, T. 2003, *ApJ*, 587, 25
- Dickinson, M., et al. 2000, *ApJ*, 531, 624
- Dubinski, J., Mihos, J. C., & Hernquist, L. 1999, *ApJ*, 526, 607
- Ferguson, H. C., et al. 2004, *ApJ*, 600, L107
- Franx, M., et al. 2003, *ApJ*, 587, L79
- Giavalisco, M. 2002, *ARA&A*, 40, 579
- Giavalisco, M., & Dickinson, M. 2001, *ApJ*, 550, 177
- Giavalisco, M., Steidel, C. C., Adelberger, K. L., Dickinson, M., Pettini, M., & Kellogg, M. 1998, *ApJ*, 503, 543
- Giavalisco, M., et al. 2004a, *ApJ*, 600, L93
- . 2004b, *ApJ*, 600, L103
- Glazebrook, K., et al. 2004, *Nature*, 430, 181
- Gonzalez-Garcia, A., & Balcells, M. 2005, *MNRAS*, 357, 753
- Gottlober, S., Klypin, A., & Kravtsov, A. V. 2001, *ApJ*, 546, 223
- Gregg, M. D., & West, M. J. 2004, in *IAU Symp. 217, Recycling Intergalactic and Interstellar Matter*, ed. P.-A. Duc, J. Braine, & E. Brinks (San Francisco: ASP), 70
- Grogin, N. A., et al. 2005, *ApJ*, 627, L97
- Hernandez, X., & Lee, W. H. 2004, *MNRAS*, 347, 1304
- Hernandez-Toledo, H. M., Avila-Reese, V., Conselice, C. J., & Puerari, I. 2005, *AJ*, 129, 682
- Hernquist, L. 1987, *ApJS*, 64, 715
- . 1993, *ApJS*, 86, 389
- Jogee, S., et al. 2004, *ApJ*, 615, L105
- Khochfar, S., & Burkert, A. 2001, *ApJ*, 561, 517
- Kodaira, K., et al. 2003, *PASJ*, 55, L17
- Kolatt, T. S., Bullock, J. S., Sigad, Y., Kravtsov, A. V., Klypin, A. A., Primack, J. R., & Dekel, A. 2000, preprint (astro-ph/0010222)
- Lacey, C., & Cole, S. 1993, *MNRAS*, 262, 627
- Lada, C. J., & Lada, E. A. 2003, *ARA&A*, 41, 57
- Lee, K., Giavalisco, M., Gnedin, O. Y., Somerville, R., Ferguson, H., Dickinson, M., & Ouchi, M. 2006, *ApJ*, in press (astro-ph/0508090)
- Le Fèvre, O., et al. 2000, *MNRAS*, 311, 565
- Lehmer, B. D., et al. 2005, *AJ*, 129, 1
- Lin, L., et al. 2004, *ApJ*, 617, L9
- Lotz, J. M., Primack, J., & Madau, P. 2004, *AJ*, 128, 163
- McCarthy, P. J., et al. 2004, *ApJ*, 614, L9
- Mihos, J. C. 2001, *ApJ*, 550, 94
- Mihos, J. C., Dubinski, J., & Hernquist, L. 1998, *ApJ*, 494, 183
- Mihos, J. C., & Hernquist, L. 1996, *ApJ*, 464, 641
- Mobasher, B., Jogee, S., Dahlen, T., de Mello, D., Lucas, R. A., Conselice, C. J., Grogin, N. A., & Livio, M. 2004, *ApJ*, 600, L143
- Moore, B., Lake, G., & Katz, N. 1998, *ApJ*, 495, 139
- Morgan, W. W. 1988, *ARA&A*, 26, 1
- Moustakas, L. A., et al. 2004, *ApJ*, 600, L131
- Nagamine, K., Cen, R., Hernquist, L., Ostriker, J. P., & Springel, V. 2005, *ApJ*, 618, 23
- Papovich, C., Dickinson, M., & Ferguson, H. C. 2001, *ApJ*, 559, 620
- Papovich, C., Dickinson, M., Giavalisco, M., Conselice, C. J., & Ferguson, H. C. 2003, *ApJ*, 598, 827
- Patton, D. R., Carlberg, R. G., Marzke, R. O., Pritchett, C. J., da Costa, L. N., & Pellegrini, P. S. 2000, *ApJ*, 536, 153
- Patton, D. R., Pritchett, C. J., Yee, H. K. C., Ellingson, E., & Carlberg, R. G. 1997, *ApJ*, 475, 29
- Patton, D. R., et al. 2002, *ApJ*, 565, 208
- Pope, A., Borys, C., Scott, D., Conselice, C. J., Dickinson, M., & Mobasher, B. 2005, *MNRAS*, 358, 149
- Press, W. H., & Schechter, P. 1974, *ApJ*, 187, 425
- Ravindranath, S., et al. 2004, *ApJ*, 604, L9
- . 2005, *ApJ*, submitted
- Rudnick, G., et al. 2003, *ApJ*, 599, 847
- Shapley, A. E., Erb, D. K., Pettini, M., Steidel, C. C., & Adelberger, K. L. 2004, *ApJ*, 612, 108
- Shapley, A. E., Steidel, C. C., Adelberger, K. L., Giavalisco, M., & Pettini, M. 2001, *ApJ*, 562, 95
- Somerville, R. S., Primack, J. R., & Faber, S. M. 2001, *MNRAS*, 320, 504
- Somerville, R. S., et al. 2004, *ApJ*, 600, L135
- Stanford, S. A., Dickinson, M., Postman, M., Ferguson, H. C., Lucas, R. A., Conselice, C. J., Budavari, T., & Somerville, R. 2004, *AJ*, 127, 131
- Steidel, C. C., Giavalisco, M., Pettini, M., Dickinson, M., & Adelberger, K. L. 1996, *ApJ*, 462, L17
- Strader, J., Brodie, J. P., & Forbes, D. A. 2004, *AJ*, 127, 3431
- Tasca, L. A. M., & White, S. D. M. 2005, *MNRAS*, submitted (astro-ph/0507249)
- Toomre, A. 1977, in *Evolution of Galaxies and Stellar Populations*, ed. B. M. Tinsley & R. B. Larson (New Haven: Yale Univ. Press), 401
- van Dokkum, P. G., et al. 2004, *ApJ*, 611, 703
- Weatherley, S. J., & Warren, S. J. 2003, *MNRAS*, 345, L29
- Windhorst, R., et al. 2002, *ApJS*, 143, 113
- Xu, C. K., Sun, Y. C., & He, X. T. 2004, *ApJ*, 603, L73
- Zepf, S. E., & Koo, D. C. 1989, *ApJ*, 337, 34